CONFIDENTIAL

Copy 187

RM A54E03

NACA

RESEARCH MEMORANDUM

FORCES AND MOMENTS ON INCLINED BODIES AT MACH NUMBERS FROM 3.0 TO 6.3

By David H. Dennis and Bernard E. Cunningham

Ames Aeronautical Laboratory
Moffett Field, Calif.

CLASSIFIED DOCUMENT

This material contains information affecting the National Defense of the United States within the meaning of the espionage laws, Title 18, U.S.C., Secs. 793 and 794, the transmission or revelation of which in any manner to an unauthorized person is prohibited by law.

NATIONAL ADVISORY COMMITTEE
FOR AERONAUTICS

WASHINGTON

June 25, 1954

CONFIDENTIAL

NACA RM A54E08 CONFIDENTIAL

NATIONAL ADVISORY COMMITTEE FOR AERONAUTICS

RESEARCH MEMORANDUM

FORCES AND MOMENTS ON INCLINED BODIES AT MACH NUMBERS FROM 3.0 TO 6.3

By David H. Dennis and Bernard E. Cunningham

SUMMARY

Results of force and moment tests at Mach numbers from 3.0 to 6.3 on bodies of revolution of fineness ratios from 5 to 10 and on flat-bottom bodies of fineness ratio 10 are presented and compared with the theoretical predictions of the crossflow method of Allen and the impact theory of Newton. Eight cone and cone-cylinder models with nose fineness ratios from 3 to 7 and afterbody fineness ratios from 2 to 7, six nose-cylinder models of fineness ratios 7 and 10 having fineness ratio 5 ogival and blunt nose shapes, and three flat-bottom bodies were tested at angles of attack to 25°. Reynolds numbers based on body diameter varied from approximately 0.1 to 0.7 million depending on test Mach number.

Comparisons of force characteristics of the various body shapes show that the forces on cylindrical afterbodies are not appreciably affected by moderate changes in the profile shape of a given fineness ratio nose. At large values of lift coefficient the lift-drag ratios of the flat-bottom shapes are higher than those of the similar cone-cylinder bodies of revolution. However, the maximum lift-drag ratios may be either higher or lower than those of the corresponding bodies of revolution, depending on nose fineness ratio and test Mach number.

Predictions of forces by the crossflow method of Allen are found to agree well with experimental results for the bodies of revolution up to a Mach number of about 4 if adequate estimates of initial lift-curve slopes are used in computing the forces. At the higher Mach numbers the experimental results for the bodies of revolution and for the flat-bottom bodies approach those predicted by the impact theory.

INTRODUCTION

At high supersonic speeds much of the lift required by an aircraft can be supplied by the body, with planar surfaces, or wings, employed for the most part for stabilization and control only. It is evident, then,

that for the design of high-speed missiles, accurate knowledge of the forces and the attendant moments acting on inclined bodies is required. In general, however, this information is not available at Mach numbers greater than about 3 since there are neither well-established theories nor any mass of experimental data for these high speeds.

In view of the absence of specific theoretical methods for high supersonic speeds, it is necessary to use either those theories which have been applied successfully at lower speeds or those which have been proposed for hypersonic speeds (i.e., $M \rightarrow \infty$). For determining the aerodynamic characteristics of inclined bodies of revolution of practical fineness ratios, the method proposed by Allen (ref. 1) has been found to be suitable at low supersonic speeds since it accounts, in at least an approximate manner, for the effects of viscous separation of the flow about bodies of revolution. The Newtonian, or impact, theory (see, e.g., ref. 2) which also accounts qualitatively for separation of the flow over the lee sides of bodies has been shown to be applicable to bodies of arbitrary shape at hypersonic speeds. To date, however, sufficient experimental data have not been obtained to ascertain the accuracy of these theories for the prediction of aerodynamic characteristics at Mach numbers from 3 to 6. As a step toward providing such test results, an experimental program to determine the aerodynamic characteristics of inclined bodies at high Mach numbers and at angles of attack up to 25° was undertaken. The first phase of this program concerned the determination of the forces and the pitching moments acting on body nose sections of fineness ratios from 3 to 7 at Mach numbers from 2.7 to 5.0. The results are reported in reference 3. The purpose of the present phase of the investigation is to determine the forces and moments on inclined nose-cylinder bodies of revolution of fineness ratios from 5 to 10 at Mach numbers from 3.0 to 6.3 and to compare these results with available theories.

In addition to the tests on bodies of revolution, a limited investigation was made to determine the effects on force characteristics - and, in particular, the effect on maximum lift-drag ratios - of changing the cross-sectional shape of bodies. The models tested were modified cone-cylinder bodies of fineness ratio 10 having flat bottom surfaces. The particular modification to provide flat-bottom shapes was investigated in view of the predictions of Sänger (ref. 4) which indicated that at hypersonic speeds, increases in lift-drag ratios as well as in lift forces would be realized by utilizing such shapes.

SYMBOLS

A	maximum cross-sectional area of body
C_D	drag coefficient, $\frac{D}{qA}$

C_{D_0}	minimum drag coefficient
ΔC_D	increment of drag coefficient $(C_D - C_{D_0})$
C_L	lift coefficient, $\frac{L}{qA}$
$\frac{dC_L}{d\alpha}$	lift-curve slope, per radian
C_m	pitching-moment coefficient about body nose, $\frac{\text{pitching moment}}{qAl}$
D	body drag
f	body fineness ratio, $\frac{l}{2r_b}$
L	body lift
M	free-stream Mach number
l	body length
q	free-stream dynamic pressure
r	body radius
r_b	maximum body radius
Re	Reynolds number, based on maximum diameter of bodies of revolution or width of flat-bottom bodies
x	axial distance measured from body nose
$\bar{x}$	center-of-pressure location, percent body length from nose
α	angle of attack

Subscripts

n	body nose
a	afterbody

EXPERIMENT

Apparatus and Tests

The tests were conducted in the Ames 10- by 14-inch supersonic wind tunnel which is of the continuous-flow, nonreturn type and operates with

a nominal supply pressure of 6 atmospheres. The Mach number in the test section may be varied from approximately 2.7 to 6.3 by changing the relative positions of the symmetrical top and bottom walls of the wind tunnel. During operation at the higher Mach numbers, the supply air is heated before entering the wind tunnel to prevent condensation of the air. A detailed description of the wind tunnel and its associated equipment and of the characteristics of the flow in the test section may be found in reference 5.

Aerodynamic forces and moments were measured with a three-component strain-gage balance. Tare forces on the sting supports were essentially eliminated by shrouds that extended to within 0.040 inch of the model base. Axial forces on the bases of the models, determined from measured base pressures and free-stream static pressures, were subtracted from measured total forces; thus, the data presented do not include the pressure forces acting on the bases of the test bodies.

Reynolds numbers based on the maximum diameters of the test bodies of revolution or widths of the flat-bottom bodies were:

Mach number	Reynolds number
3.0	0.59×10^{6}
3.5	.71
4.2	.54
5.0	.26
6.3	.11

Reynolds numbers based on body lengths may be obtained by multiplying the above values by model fineness ratios.

Models

The body shapes tested in the present investigation are shown in figure 1. To determine the effects of varying the afterbody length of bodies of given nose fineness ratios and of varying the nose fineness ratio of bodies of given over-all fineness ratios, the series of cone and cone-cylinder models shown in figure 1(a) were tested. These bodies are: fineness ratio 3 cones with 2, 4, and 7 diameter long cylindrical afterbodies; fineness ratio 5 cone and $f_n = 5$ cones with 2 and 5 diameter long afterbodies; a fineness ratio 7 cone and an $f_n = 7$ cone with a 3 diameter long afterbody.

To determine the effects of varying nose-profile shape on the aerodynamic characteristics of bodies, the models shown in figure 1(b) were tested. These fineness ratio 5 nose shapes are: a tangent ogive, a

parabola of revolution, and a so-called 3/4-power nose.[1] The 3/4-power nose has been shown to be an approximation to the nose shape of given fineness ratio having minimum drag at hypersonic speeds (ref. 6) and was found to retain its low drag advantage at angles of attack (ref. 3). In the present investigation these shapes were tested with fineness ratio 2 cylindrical afterbodies, as shown in the photograph, and with fineness ratio 5 afterbodies. The test bodies of revolution have base diameters of 3/4 inch.

The effects of one variation of body cross-section shape were investigated by testing the modified cone-cylinder models shown in figure 1(c). These bodies have flat bottoms and are of D shaped cross section with the top portions of the noses and the top portions of the afterbodies being half-circular, as shown in the sketch (fig. 1(d)). The nose fineness ratios of the flat-bottom bodies are 3, 5, and 7. The total fineness ratio of all three bodies is 10.

Accuracy of Test Results

Variations of Mach number in the region of the test section where the models were located did not exceed ±0.02 from the mean values[2] except at Mach number 6.3 where the variation was ±0.04. Variations of free-stream Reynolds number from the values given previously did not exceed $\pm 0.02 \times 10^6$.

The estimated errors in angle-of-attack values due to uncertainties in corrections for stream angle and for deflections of the model support system were $\pm 0.2^\circ$.

Precision of the experimental results was affected both by uncertainties in the measurements of the forces by the balance system and by uncertainties in the determination of free-stream dynamic pressures and base pressures. At the high angles of attack, these uncertainties result in maximum possible errors in lift and drag coefficients of ±0.020 at Mach numbers from 3.0 to 5.0 and ±0.045 at Mach number 6.3. At angles

[1]It may be noted that the cone is a member of the same family of shapes as the parabola and the 3/4-power shape, the expression defining these shapes being

$$r = r_b \left(\frac{x}{l_n}\right)^m$$

where m = 1 for the cone and m = 3/4 and m = 1/2 for the 3/4-power and the parabolic shapes, respectively.

[2]The nominal Mach numbers of 3.0, 3.5, 4.2, 5.0, and 6.3 used for simplicity in this paper correspond to actual mean values of 3.01, 3.49, 4.24, 5.04, and 6.28, respectively.

of attack less than about 10°, the corresponding maximum errors are ±0.015 and ±0.030, respectively. Possible errors in pitching-moment coefficients were ±0.020 at the lower Mach numbers and ±0.045 at Mach number 6.3. It should be pointed out that the above discussion concerns estimated magnitudes of the maximum possible errors and it is believed that, in general, the errors in the results presented are much less than the foregoing estimates.

RESULTS AND DISCUSSION

Because only typical results are presented in the following discussion and many of the data obtained in the present tests are not shown in graphical form, all of the experimental results are presented in table I. Lift, drag, and pitching-moment coefficients, centers of pressure, and lift-drag ratios at the several test Mach numbers are tabulated for each of the 17 test bodies at the various angles of attack.

The following discussion is presented in two parts. The first section concerns variations of the experimentally determined characteristics of the bodies with changes in Mach number and in body shape. In the second part, comparisons of theoretical predictions with the test results are discussed.

Test Results

Effects of Mach number variation.- In the Mach number range from 3 to 5, the initial lift-curve slopes ($dC_L/d\alpha$ at $\alpha = 0$) for the bodies of revolution tested generally increase with increasing Mach number. For each of the models this increase (shown for three of the models at the top of fig. 2) is larger than would be expected for the noses alone in this Mach number range and may be attributed, in part, to the increase in lift carry-over on the cylindrical afterbodies.

The increase in initial lift-curve slopes up to $M = 5.0$ is reflected in the variations of lift coefficient with Mach number (fig. 2) at $\alpha = 5°$. At the higher angles of attack, however, the variations of C_L with Mach number are no longer similar to the variation of initial lift-curve slope. This change in the variations of lift coefficients occurs because the lift is due, in large part, to the effects of viscous separation of the flow over the lee sides of the bodies.

Variations of center-of-pressure positions with Mach number for the three fineness ratio 10 cone-cylinder bodies are shown in figure 3. At the low angles of attack (2° and 5°), the centers of pressure move aft with increasing Mach number. This characteristic may, as with the

variation of lift-curve slopes, be attributed to the increasing lift carry-over on the cylindrical afterbodies with increasing Mach number. At the high angles of attack, the forces result, in large part, from the effects of viscous separation, and the center-of-pressure positions are comparatively unaffected by Mach number variations. This indicates that the distribution of force due to separation is relatively independent of Mach number.

Effects of adding cylindrical afterbody to a conical nose.- In figure 4 are shown the variations with cylindrical-afterbody length of lift coefficient at several angles of attack and of maximum lift-drag ratios for the cone-cylinder bodies tested at Mach number 3.0.[3] At 2° angle of attack, viscous separation of the flow over the lee side of the body does not occur to an appreciable extent; hence the addition of cylindrical afterbody in excess of 2 to 3 diameters results in essentially no further increase in lift coefficient. This occurs because the inviscid lift carry-over on the cylindrical afterbody decreases with distance downstream of the nose-cylinder juncture. At high angles of attack, where the viscous cross forces contribute a large part of the lift, the lift coefficients increase approximately uniformly with cylindrical afterbody length. The slightly greater rate of increase for the short cylindrical afterbodies may be attributed in part to the inviscid lift carry-over effect and in part to the nonuniform distribution of the viscous cross forces over the forward portions of bodies (see e.g., ref. 7).

Maximum lift-drag ratios are increased by the additions of afterbodies, the greatest increase occurring for the fineness ratio 3 cone. Addition of a 3 diameter cylindrical afterbody to the fineness ratio 7 cone has a relatively small effect, and it is apparent that longer afterbodies would not appreciably increase the maximum lift-drag ratio.

Effect of changing nose shape of nose-cylinder bodies.- The variations in aerodynamic characteristics of the test noses alone were discussed in detail in reference 3. It was found in the present tests that the differences in characteristics among test bodies differing only in nose shape were approximately the same as the differences that were found among the noses alone. That is, the addition of a 2 or 5 diameter long cylinder to a fineness ratio 5 nose has approximately the same effect irrespective of the nose shape. This is illustrated in figure 5 where it may be seen that the variation of lift coefficient with cylinder length is approximately the same for the four nose shapes investigated. (The data for the noses alone have been taken from results at $M = 2.75$ presented in reference 3.) Although the bodies having the 3/4-power nose shape retain the advantage of higher lift-drag ratios than the bodies with other nose shapes, the addition of a cylindrical afterbody results in approximately the same increases in lift and in drag irrespective of

[3]The values for the fineness ratio 3 cone (zero cylinder length) were taken from the data at $M = 2.75$ of reference 3. These data were corrected to account for the small change in test Mach number.

nose profile shape, and the differences in maximum lift-drag ratios are decreased somewhat by the addition of afterbody as shown at the top of figure 5.

Effects of varying nose fineness ratio on bodies of constant over-all fineness ratio.- For bodies of equal over-all fineness ratio, increasing nose fineness ratio results in decreases in the initial lift-curve slope and in the lift coefficients at any angle of attack. This is illustrated in figure 6 for the fineness ratio 10 cone-cylinder bodies at Mach number 4.2. As a result of the decrease in wave drag accompanying the increase in nose fineness ratio, there is a large gain in the maximum lift-drag ratio. The increased $(L/D)_{max}$ is, however, accompanied by a decrease in the lift coefficient at $(L/D)_{max}$.

The axial movements of the centers of pressure of the fineness ratio 10 bodies with increasing lift coefficient are similar, as can be seen in figure 6. Moreover, the centers of pressure are approximately the same distance forward of the centers of volume of the bodies. For example, at a lift coefficient of 1.4, all of the centers of pressure are 11 to 12 percent of body lengths forward of the respective centers of volume.

Flat-bottom ("D") bodies.- Aerodynamic characteristics typical of the flat-bottom bodies tested are shown in figure 7. The variations with angle of attack of the lift, drag, and pitching-moment coefficients and the center-of-pressure positions are shown for the D body with a fineness ratio 5 nose at Mach number 4.2. It can be seen that within the angle-of-attack range from -10° to $+24^\circ$, no erratic variations of forces or of pitching moment occur. However, as would be expected because of the nonsymmetrical profile shape of the body, zero lift, zero pitching moment, and minimum drag occur at small positive angles of attack. At angles of attack near zero lift, a nose-down couple exists which causes the center-of-pressure position to vary from an infinite distance upstream to an infinite distance downstream of the nose as α is increased through the angle for zero lift. However, the center-of-pressure position does not shift appreciably with angle of attack outside the range from approximately -4° to approximately $+8^\circ$.

Although not shown in figure 7, the angle of attack for zero lift on the D bodies increases with increasing Mach number. For the test body just discussed, this shift is from $\alpha = 1^\circ$ at $M = 3.0$ to $\alpha = 3^\circ$ at $M = 6.3$.

Typical curves of the force characteristics of the flat-bottom bodies and of the cone-cylinder bodies of revolution having the same nose and over-all fineness ratios are shown in figure 8 for three different Mach numbers. It should be noted that because the base area of the D bodies is greater than that of the cone-cylinders, ratios of the force coefficients at given test conditions do not show directly the relationships of the forces on the two types of bodies. (However, the ratio of base areas is the same as the ratio of body volumes, thus the coefficients as presented are a direct measure of the forces per unit body volume.)

The results shown in figure 8 indicate that the minimum drag coefficients are generally slightly lower for the cone-cylinder bodies than for the corresponding D bodies. However, the rate of drag rise is lower for the D bodies. These differences are reflected in the lift-drag-ratio curves where it is seen that, in general, the lift-drag ratios of the cone-cylinders are higher than those of the flat-bottom bodies at low lift coefficients whereas the reverse is true at high lift coefficients. Furthermore, maximum lift-drag ratios occur at lower values of C_L for the cone-cylinder bodies than for the D bodies. It is apparent then that, as shown in figure 8(a), for conditions where the zero-lift drags of both bodies are relatively low, the body of revolution has the higher maximum lift-drag ratio. Conversely, as shown in figure 8(c), for fineness ratios and test conditions resulting in high zero-lift drags, the D body has the higher $(L/D)_{max}$. For intermediate conditions (fig. 8(b)) both bodies have approximately the same maximum lifting efficiency. An experimental investigation at Mach number 6.86 (ref. 8) was conducted on shapes very similar to the flat-bottom body and cone-cylinder body of intermediate nose fineness ratios employed in the present tests. While in the present investigation the two bodies were found to have approximately the same values of $(L/D)_{max}$ at $M = 3.0$ (fig. 8(b)), the results of the tests of the similar bodies at $M = 6.86$ show that the D body has the higher $(L/D)_{max}$. Although, under some conditions the flat-bottom body may be more efficient than the body of revolution, this advantage may be offset by the probable unstable roll characteristics associated with such a shape.

Visual flow studies.- A limited investigation of the flow about two of the fineness ratio 10 cone-cylinder test bodies was conducted by means of the vapor-screen technique to determine if the characteristics of the flow about inclined bodies of revolution at Mach numbers of about 4 are similar to those observed heretofore at lower Mach numbers. A description of this experimental method and of the observations made may be found in reference 9. A more complete description of the flow about a large number of bodies at $M = 2$ observed by the same technique may be found in reference 10. During the present tests, observations were made only at angles of attack of 15°, 20°, and 25° on the cone-cylinder bodies having nose fineness ratios of 3 and 7 with 7 and 3 diameter long afterbodies, respectively. The Mach numbers for these tests were from 3.0 to approximately 4.4.[4] A sketch of a vapor-screen photograph is shown in figure 9(a) to indicate the location of the vortices and the trace of the bow shock wave in the plane of the light beam that is projected through the wind tunnel. It should be noted that the model is yawed in the horizontal plane for these photographs rather than in the vertical plane as shown in references 9 and 10.

[4]The amount of condensed water vapor necessary for visual observation of the flows is sufficient to reduce somewhat the free-stream Mach numbers from the values given above which are those that exist without condensation.

While the present observations were very limited in scope, the results do serve to indicate that the flow characteristics at these Mach numbers are generally similar to those previously reported at a Mach number of 2. For example, at 15° angle of attack a steady symmetrical vortex pair existed along the entire length of the bodies (fig. 9(b)). At the higher angles of attack (20° to 25°) an unsteady configuration of approximately 4 to 6 vortices was observed over most of the body length (figs. 9(c) and 9(d)). These angles of attack are somewhat lower than those at which this unsteady vortex pattern was observed at Mach numbers of about 2. No appreciable variations in the vortex flow patterns were evident during the present tests while the Mach number was varied from 3.0 to about 4.4.

An interesting phenomenon was observed during the vapor-screen tests. This was the appearance of striations in the vapor screen when an excess of water was present in the wind-tunnel supply air. These striations are shown in figures 9(b) and 9(c) where it can be seen that the flow about the test model alters the otherwise relatively uniform appearance of the vertical striations. This characteristic, in addition to the fact that the pattern was not altered by changes in the angle or the longitudinal position of the light beam relative to the test section, indicates that the phenomenon is not associated with the optical properties of the test setup but is inherent in the flow itself. The particular reason for the unique distribution of condensed particles in the flow is as yet unexplained. For the motion picture sequence (fig. 9(d)), the amount of water vapor in the supply air was reduced sufficiently to eliminate the striations.

Comparison of Theory with Experiment

Cone-cylinder bodies of revolution.- The experimentally determined lift and drag characteristics of several of the cone-cylinder test bodies are compared in figures 10 to 13 with the predictions of Allen's crossflow method (ref. 1) and, for some cases, with the impact theory of Newton.

Because the crossflow method of reference 1 does not include the evaluation of drag at zero lift and the impact theory predictions of $C_{D(\alpha=0)}$ are generally low at the Mach numbers of interest here, only the increments of drag due to lift are compared. There are, of course, various adequate methods available for estimating the drag at zero lift of bodies of revolution. (See e.g., reference 11 for a discussion of theories for computing pressure drag, and references 12 and 13 for skin-friction drag.)

In computing the aerodynamic forces by Allen's method, the estimates of the inviscid flow contributions to the forces on the bodies were

obtained with Van Dyke's hybrid theory[5] (ref. 14) since the slender-body-theory result for initial lift-curve slope ($dC_L/d\alpha$ at $\alpha = 0$) used in reference 1 is not adequate for the Mach number range and the body shapes under consideration here. Although modifications to Allen's method for estimating the viscous effects have been suggested (see, e.g., refs. 15 and 16), for the present comparisons Allen's method was used as originally proposed.

The estimates made with the cross flow method for the fineness ratio 10 and the fineness ratio 7 cone-cylinder bodies are compared with $M = 3.0$ experimental results in figures 10 and 11, respectively. It can be seen that the estimates of lift and drag rise are very close to the measured values for the fineness ratio 10 cone-cylinders and for the fineness ratio 7 cone. However, for the $f = 7$ cone-cylinder bodies, the estimates of lift and drag rise are higher than the measured values. This overestimation of forces occurs because the predictions made with the hybrid theory of initial lift-curve slope are too high for bodies having relatively short cylindrical afterbodies, as can be shown by analysis of the data obtained during the present tests. The experimentally determined initial lift-curve slopes were used in conjunction with the same estimates of the viscous effects, and the results of this modified method agree very well with the experimental results up to angles of attack of about 20° as shown in figure 11. It appears then that in spite of the approximate nature of the crossflow method for estimating the viscous effects, the combination of this method with adequate predictions of initial lift-curve slopes provides a relatively accurate means for estimating the lift and drag-rise characteristics for a variety of cone-cylinder body shapes at Mach number 3.0. Comparisons of the experimental results with theory at Mach number 4.2 (not presented) lead to a similar conclusion.

As shown in figures 12 and 13, however, for the same body shapes at Mach number 5, this method fails, in general, to predict adquately the forces even with the experimental values of the initial lift-curve slopes. Since the crossflow method for estimating viscous effects should be as adequate at Mach number 5 as at the lower Mach numbers, the assumption of a linear variation with angle of attack of the inviscid contribution is believed to be incorrect at the higher Mach numbers.

It is shown in figures 12 and 13 that the impact-theory predictions are very close to the measured increments of drag throughout the angle-of-attack range and to the measured lift at the higher angles of attack. The initial lift-curve slopes and the calculated lift coefficients in the low angle-of-attack range are lower than measured (except in the case of

over

[5]The forces calculated with Van Dyke's theory are assumed to act in a direction normal to the body axis rather than midway between the normals to the free-stream direction and the body axis as required by the slender-body theory. Within the assumptions of the crossflow method, (i.e., $\cos \alpha = 1$) this difference does not affect the lift curves but does effectively double the inviscid contribution to the estimated drag due to lift.

the fineness ratio 7 cone) because the impact theory fails to account for the lift carry-over, or interference effects of the noses, on the afterbodies. In applying the impact theory it is assumed that zero pressure coefficient exists on the lee, or "shaded," portions of a body surface; thus for inclined bodies at high free-stream Mach numbers the theory accounts, at least approximately, for the actual flow conditions over the bodies. In general, then, it is apparent that at high angles of attack the force characteristics approach the predictions of the impact theory as the free-stream Mach number is increased ($M \sim 5$).

Comparisons of the theoretical and experimental center-of-pressure positions are shown for six of the cone-cylinder models at Mach number 3.0 and at Mach number 5.0 in figures 14 and 15, respectively. It can be seen that each theoretical method provides a fairly accurate estimate for certain cases but fails to predict adequately the centers of pressure for the full ranges of Mach number, angle of attack, and body shape.

Flat-bottom bodies.- The experimentally determined variations of lift coefficient, increment of drag coefficient, and center of pressure with angle of attack for the three flat-bottom bodies are compared in figure 16 with the predictions made with the impact theory. Experimental results are shown for Mach numbers of 3.0, 4.2, and 6.3. The agreement between predicted and measured lift improves with increasing Mach number throughout the test angle-of-attack range for the three bodies, and the agreement for the most slender configurations tested (fig. 16(c)) becomes quite good at $M = 6.3$. It can be seen that, particularly at the lower Mach numbers, angles of attack for zero lift are lower than predicted. This difference results, for the most part, because the theory fails to consider the expansion of the flow at the nose-afterbody juncture and the subsequent negative pressure coefficients on the upper surfaces of the afterbodies. As with the cone-cylinder bodies of revolution, this effect decreases with increasing nose fineness ratio.

In view of the discrepancies between the measured and predicted values of lift coefficients, the consistently good agreement between the experimental and calculated values of increment of drag coefficient at the lower Mach numbers must be considered fortuitous. It should be noted that, as for the bodies of revolution, the impact theory underestimates the minimum pressure drag for these bodies. Unfortunately, at the present there is no adequate method for estimating the drag of these body shapes at zero angle of attack for the Mach numbers of interest here.

The incorrect predictions of the angles of attack for zero lift are reflected in the curves of figure 16 showing the comparisons of the estimated and experimentally determined center-of-pressure positions. However, at the higher angles of attack where this uncertainty does not affect the results, the estimated centers of pressure are generally within approximately 1/3 body diameter of the experimentally determined positions. At the high angles the predicted position is approximately at the

center of body plan-form area. As for the variation of lift with angle of attack, the theoretical predictions generally improve with increasing Mach number and body-nose fineness ratio.

CONCLUSIONS

Analysis of the results of tests on inclined bodies of revolution and flat-bottom bodies in the Ames 10- by 14-inch supersonic wind tunnel at Mach numbers from 3.0 to 6.3 has led to the following conclusions:

1. Within the limits of body shapes tested, aerodynamic forces on cylindrical afterbodies are not appreciably affected by moderate changes in the profile shape of a body nose of given fineness ratio.

2. Increasing the nose fineness ratio of cone-cylinder bodies of given over-all fineness ratio results in increases in maximum lift-drag ratio and decreases of lift throughout the test angle-of-attack range but has little effect on the center-of-pressure positions relative to the positions of body centers of volume.

3. Although the drag at zero lift of the flat-bottom bodies is generally slightly higher, the induced drag, or drag due to lift, is lower than that of the comparable cone-cylinder bodies of revolution. Thus, the lift-drag ratios of the flat-bottom bodies are lower than those of the corresponding cone-cylinder bodies at low lift coefficients and are higher at high values of lift coefficient.

4. The method proposed by Allen for estimating the lift and increment of drag characteristics of inclined bodies of revolution adequately predicts these characteristics at Mach numbers up to about 4 if accurate values of initial lift-curve slope are used.

5. The force characteristics of the bodies of revolution at high angles of attack and of the flat-bottom bodies throughout the test angle-of-attack range approach the predictions of the impact theory as the free-stream Mach number is increased.

6. The flow about inclined bodies of revolution, that is, the distribution of vortices in the flow in the lee of the bodies, at Mach numbers from 3.0 to about 4.4 does not differ appreciably from that previously observed by others at Mach numbers of about 2.

Ames Aeronautical Laboratory
National Advisory Committee for Aeronautics
Moffett Field, Calif., May 3, 1954

REFERENCES

1. Allen, H. Julian: Estimation of the Forces and Moments Acting on Inclined Bodies of Revolution of High Fineness Ratio. NACA RM A9I26, 1949.

2. Grimminger, G., Williams, E. P., and Young, G. B. W.: Lift on Inclined Bodies of Revolution in Hypersonic Flow. Jour. Aero. Sci., vol. 17, no. 11, Nov. 1950, pp. 675-690.

3. Dennis, David H., and Cunningham, Bernard E.: Forces and Moments on Pointed and Blunt-Nosed Bodies of Revolution at Mach Numbers From 2.75 to 5.0. NACA RM A52E22, 1952.

4. Sänger, Eugen, and Bredt, J.: A Rocket Drive for Long Range Bombers. Bur. Aero., Navy Dept. CGD-32. Trans. from (ZWB Berlin-Aldershop) UM 3538. (Deutche Forschungsanstalt für Segelfulg E. V. Ernst Udet), Ainring, Aug. 1944.

5. Eggers, A. J., Jr., and Nothwang, George J.: The Ames 10- by 14-Inch Supersonic Wind Tunnel. NACA TN 3095, 1954.

6. Eggers, A. J., Jr., Dennis, David H., and Resnikoff, Meyer M.: Bodies of Revolution for Minimum Drag at High Supersonic Airspeeds. NACA RM A51K27, 1952.

7. Perkins, Edward W., and Kuehn, Donald M.: Comparison of the Experimental and Theoretical Distributions of Lift on a Slender Inclined Body of Revolution at M = 2.0. NACA RM A53E01, 1953.

8. Ridyard, Herbert W.: The Aerodynamic Characteristics of Two Series of Lifting Bodies at Mach Number 6.86. NACA RM L54C15, 1954.

9. Allen, H. Julian, and Perkins, Edward W.: Characteristics of Flow Over Inclined Bodies of Revolution. NACA RM A50L07, 1951.

10. Gowen, Forrest E., and Perkins, Edward W.: A Study of the Effects of Body Shape on the Vortex Wakes of Inclined Bodies at a Mach Number of 2. NACA RM A53I17, 1953.

11. Ehret, Dorris M.: Accuracy of Approximate Methods for Predicting Pressures on Pointed Nonlifting Bodies of Revolution in Supersonic Flow. NACA TN 2764, 1952.

12. Van Driest, E. R.: Investigation of Laminar Boundary Layer in Compressible Fluids Using the Crocco Method. NACA TN 2597, 1952.

13. Chapman, Dean R., and Kester, Robert H.: Measurements of Turbulent Skin Friction on Cylinders in Axial Flow at Subsonic and Supersonic Velocities. Jour. Aero. Sci., vol. 20, no. 7, July 1953, pp. 441-448.

14. Van Dyke, Milton D.: First- and Second-Order Theory of Supersonic Flow Past Bodies of Revolution. Jour. Aero. Sci., vol. 18, no. 3, Mar. 1951, pp. 161-178, 216.

15. Hill, J.A. F.: Forces on Slender Bodies at Angles of Attack. Mass. Inst. of Tech., Naval Supersonic Laboratory, R-a 100-59, May 9, 1950.

16. Kelley, Howard R.: The Estimation of Normal Force and Pitching Moment Coefficients for Blunt-Based Bodies of Revolution at Large Angles of Attack. U. S. Naval Ordnance Test Station, Inyokern, Calif., Tech. Memo. 998, May 27, 1953.

TABLE I.- EXPERIMENTAL RESULTS

M	α	C_L	C_D	$\frac{L}{D}$	C_m	$\bar{x}$	M	α	C_L	C_D	$\frac{L}{D}$	C_m	$\bar{x}$
(a) f_n = 3 cone, f_a = 2 cylinder													
3.01	-2.0	-0.094	0.112	-0.84	0.056	57	5.04	-2.0	-0.094	0.114	-0.82	0.049	50
	0	0	.112	0	- - -	--		0	0	.113	0	- - -	--
	1.0	.046	.116	.40	- - -	--		1.0	.042	.114	.37	- - -	--
	2.0	.088	.117	.75	-.049	53		1.8	.078	.121	.64	- - -	--
	3.3	.165	.118	1.40	-.093	54		3.3	.242	.136	1.78	-.131	52
	4.1	.184	.123	1.50	-.095	49		7.3	.342	.159	2.15	-.196	54
	7.4	.387	.160	2.42	-.222	55		9.3	.451	.190	2.37	-.272	57
	10.2	.553	.211	2.62	-.315	54		12.1	.583	.267	2.18	-.357	57
	11.4	.648	.245	2.64	-.389	57		14.1	.698	.321	2.17	-.433	57
	14.3	.846	.325	2.60	-.506	56		16.1	.812	.388	2.09	-.524	59
	17.4	1.054	.442	2.38	-.663	58		19.3	.939	.503	1.87	-.609	58
	18.4	1.155	.502	2.30	-.715	57		21.3	1.051	.607	1.73	-.703	59
	21.4	1.339	.651	2.06	-.859	58		23.3	1.157	.711	1.63	-.786	59
	25.4	1.602	.921	1.74	-1.090	59							
(b) f_n = 3 cone, f_a = 4 cylinder													
3.01	-2.0	-.093	.121	-.77	.039	40	5.04	-2.0	-.080	.131	-.61	.031	37
	0	0	.102	0	- - -	--		0	0	.127	0	0	--
	1.0	.048	.110	.44	-.019	38		1.0	.049	.128	.38	-.025	48
	2.0	.097	.117	.83	-.041	40		1.8	.082	.122	.67	-.044	51
	3.8	.198	.134	1.48	-.089	44		5.8	.316	.140	2.26	-.174	53
	4.1	.205	.127	1.61	-.090	42		7.8	.448	.170	2.63	-.250	54
	7.9	.488	.192	2.54	-.246	48		9.8	.587	.212	2.77	-.324	53
	10.2	.709	.249	2.85	-.368	50		12.1	.760	.298	2.55	-.430	53
	12.0	.891	.315	2.83	-.491	52		14.1	.916	.381	2.48	-.521	53
	14.4	1.147	.414	2.77	-.636	52		16.1	1.061	.479	2.22	-.610	52
	17.5	1.495	.607	2.46	-.853	53		19.3	1.361	.676	2.01	-.822	54
	18.5	1.590	.636	2.50	-.905	53		21.3	1.534	.815	1.88	-.944	55
	21.5	1.888	.899	2.10	-1.097	53		23.3	1.710	.971	1.76	-1.060	54
4.24	-2.0	-.100	.110	-.91	- - -	--	6.28	-2.0	-.079	.218	-.36	- - -	--
	0	0	.105	0	- - -	--		0	0	.208	0	- - -	--
	1.0	.040	.108	.37	- - -	--		1.0	.040	.202	.20	- - -	--
	2.0	.096	.121	.79	- - -	--		2.0	.085	.204	.41	- - -	--
	4.8	.254	.118	2.15	-.147	56		6.0	.309	.227	1.36	-.158	48
	7.8	.470	.166	2.83	-.260	53		7.8	.433	- - -	- - -	-.213	47
	10.4	.663	.231	2.87	-.867	53		9.8	.566	- - -	- - -	-.301	49
	11.2	.752	.262	2.87	-.424	54		12.1	.732	.370	1.98	-.397	50
	14.2	1.003	.376	2.67	-.586	55		14.1	.892	.454	1.97	-.483	50
	16.2	1.169	.472	2.48	-.686	55		16.1	1.086	.561	1.94	-.625	52
	18.4	1.327	.607	2.19	-.784	54		19.3	1.377	.780	1.77	-.834	54
	21.4	1.578	.813	1.94	-.959	54		21.3	1.567	.930	1.69	-.978	54
	23.9	1.796	1.018	1.76	-1.122	55		23.3	1.762	1.097	1.61	-1.150	56
(c) f_n = 3 cone, f_a = 7 cylinder													
3.01	-2.1	-.104	.162	-.64	- - -	--	4.24	4.3	.293	.150	1.95	-.117	38
	0	0	.158	0	0	--		7.4	.557	.202	2.76	-.250	43
	1.0	.054	.167	.32	-.018	31		10.4	.877	.285	3.08	-.413	45
	2.1	.109	.170	.64	-.037	32		11.4	1.013	.321	3.16	-.513	49
	3.4	.189	.178	1.06	-.064	32		14.3	1.344	.479	2.81	-.678	48
	4.1	.229	.174	1.32	-.077	32		14.4	1.388	.480	2.89	-.700	48
	7.5	.507	.231	2.19	-.197	37		16.5	1.617	.607	2.66	- - -	--
	10.4	.919	.312	2.81	-.408	42		18.5	1.913	- - -	- - -	-1.011	49
	11.7	1.083	.386	2.92	-.503	44		21.5	2.353	1.054	2.23	-1.303	51
	14.6	1.573	.538	2.95	-.768	46		24.1	2.750	1.363	2.02	-1.582	52
	17.7	1.908	.763	2.50	- - -	--							
	18.9	2.235	.920	2.43	-1.165	48	5.04	-2.0	-.107	.165	.65	.041	37
								0	0	.151	0	0	--
3.49	-2.1	-.115	.152	-.76	- - -	--		1.0	.056	.152	.37	-.021	35
	0	0	.149	0	0	--		1.8	.099	.156	.63	-.039	37
	1.0	.057	.155	.37	-.020	33		5.3	.376	.196	1.92	-.141	36
	2.1	.116	.154	.75	-.041	34		7.3	.570	.247	2.31	-.269	45
	3.4	.211	.164	1.29	-.077	35		9.3	.763	.308	2.48	-.362	45
	4.1	.248	.165	1.50	-.090	35		12.3	1.018	.372	2.74	-.460	43
	7.5	.554	.221	2.51	-.202	40		14.3	1.246	.478	2.61	-.596	45
	10.4	.952	.307	3.10	-.460	46		16.3	1.454	.595	2.44	-.748	48
	10.5	.986	.302	3.26	-.472	46		21.4	2.041	1.026	1.99	-1.031	46
	11.7	1.067	.350	3.05	-.513	46		23.4	2.272	1.218	1.86	-1.215	47
	14.6	1.528	.527	2.90	-.772	48	6.28	-2.0	-.097	- - -	- - -	- - -	--
	14.7	1.560	.521	2.99	-.776	47		0	0	- - -	- - -	- - -	--
	17.7	1.972	.810	2.44	- - -	--		1.0	.048	- - -	- - -	- - -	--
	18.8	2.121	.874	2.43	-1.120	49		2.0	.091	- - -	- - -	- - -	--
								5.3	.338	.225	1.50	- - -	--
4.24	-2.0	-.110	.138	-.80	- - -	--		7.3	.511	.270	1.89	- - -	--
	0	0	.125	0	0	--		9.3	.700	.338	2.07	- - -	--
	1.0	.052	.133	.39	-.011	21		12.2	.990	.475	2.08	-.483	45
	2.0	.112	.143	.78	-.031	27		14.2	1.236	.586	2.11	-.622	46
								16.2	1.469	.719	2.04	-.771	48

TABLE I.- EXPERIMENTAL RESULTS - Continued

M	α	C_L	C_D	$\frac{L}{D}$	C_m	$\bar{x}$	M	α	C_L	C_D	$\frac{L}{D}$	C_m	$\bar{x}$
(d) f_n = 5 cone													
3.01	-2.0	-0.063	0.076	-0.83	0.042	64	5.04	-2.0	-0.068	- - -	- - -	0.046	68
	0	0	.071	0	0	--		0	.003	- - -	- - -	- - -	--
	1.0	.029	.066	.44	-.022	70		1.0	.035	- - -	- - -	- - -	--
	2.0	.062	.073	.85	-.038	59		2.0	.070	- - -	- - -	-.049	70
	3.3	.109	.066	1.65	-.076	67		3.3	.173	.105	1.65	-.122	67
	7.3	.263	.089	2.95	-.184	67		7.3	.249	.115	2.16	-.178	68
	10.1	.392	.124	3.16	-.276	67		9.3	.332	.140	2.37	-.238	68
	11.4	.473	.147	3.22	-.333	68		12.1	.466	.179	2.49	-.334	68
	14.2	.628	.221	2.84	-.440	66		14.1	.559	.229	2.44	-.389	65
	17.3	.796	.306	2.60	- - -	--		16.1	.658	.289	2.28	-.471	66
	18.3	.877	.359	2.44	-.631	67		19.3	.800	.410	1.95	- - -	--
	21.3	1.017	.475	2.14	- - -	--		21.3	.890	.491	1.81	- - -	--
	25.4	1.236	.687	1.80	- - -	--		23.3	.975	.584	1.67	- - -	--
(e) f_n = 5 cone, f_a = 2 cylinder													
3.01	-2.0	-.086	.079	-1.09	- - -	--	4.24	4.3	.184	.062	2.97	- - -	--
	0	0	.070	0	0	--		7.3	.351	.096	3.66	- - -	--
	1.0	.038	.075	.51	-.019	--		9.3	.491	.140	3.51	- - -	--
	2.0	.081	.084	.96	-.047	56		11.2	.657	.184	3.57	-.406	60
	3.3	.144	.076	1.89	-.087	59		14.3	.884	.288	3.07	-.549	59
	4.0	.170	.091	1.86	-.094	53		16.3	1.025	.370	2.77	-.640	59
	7.3	.366	.105	3.49	-.225	60		18.3	1.139	.483	2.36	-.753	61
	10.3	.602	.164	3.52	-.375	60		21.4	1.364	.651	2.09	-.911	61
	11.4	.684	.190	3.60	-.421	60		23.9	1.452	.806	1.91	-1.054	61
	14.4	.986	.300	3.29	-.611	59							
	17.4	1.240	.452	2.74	-.809	61	5.04	-2.0	-.085	.086	-.99	- - -	--
	18.5	1.368	.521	2.63	- - -	--		0	0	.078	0	- - -	--
	21.4	1.614	.714	2.26	-1.079	61		1.0	.048	.074	.65	- - -	--
	23.5	1.792	.872	2.06	-1.215	61		1.8	.087	.074	1.18	- - -	--
								5.3	.246	.088	2.68	- - -	--
4.24	-2.0	-.083	.058	-1.43	- - -	--		7.3	.341	.114	3.04	- - -	--
	0	0	.051	0	- - -	--		9.3	.471	.153	3.08	- - -	--
	1.0	.039	.062	.63	- - -	--		12.2	.649	.229	2.84	-.417	61
	2.0	.075	.059	1.27	- - -	--		14.2	.788	.297	2.65	-.508	61
								16.2	.920	.376	2.45	-.582	59
(f) f_n = 5 cone, f_a = 5 cylinder													
3.01	-2.0	-.071	.098	-.72	- - -	--	4.24	11.2	.898	.232	3.87	-.492	53
	0	0	.091	0	- - -	--		14.3	1.243	.371	3.35	-.702	54
	1.0	.045	.102	.44	-.018	38		16.3	1.479	.487	3.04	-.850	55
	2.0	.092	.103	.89	-.036	37		21.5	2.219	.967	2.30	1.376	57
	4.1	.196	.109	1.80	-.082	40		23.5	2.470	1.182	2.09	1.555	57
	4.3	.228	.106	2.15	-.098	42							
	7.4	.468	.140	3.34	-.236	49	5.04	-2.0	-.100	.082	-1.22	- - -	--
	10.3	.797	.222	3.59	-.410	50		0	0	.078	0	- - -	--
	11.6	1.004	.279	3.60	-.572	55		1.0	.052	.068	.76	- - -	--
	14.5	1.420	.419	3.39	-.781	53		1.8	.087	.082	1.06	- - -	--
	18.7	2.037	.748	2.72	-1.170	54		5.3	.307	.110	2.79	-.168	53
								7.3	.471	.143	3.29	-.263	54
3.49	-2.0	-.101	.086	-1.17	.046	44		9.3	.651	.191	3.41	-.364	54
	0	0	.089	0	0	--		12.2	.935	.285	3.28	-.531	54
	1.0	.049	.096	.51	-.023	45		14.2	1.136	.369	3.08	-.648	54
	2.0	.100	.098	1.02	-.044	43		16.2	1.347	.472	2.85	-.769	54
	3.3	.192	.094	2.04	-.095	48		19.4	1.774	.707	2.51	-1.056	55
	4.1	.202	.106	1.91	-.092	44		21.4	2.045	.885	2.31	-1.240	56
	7.4	.511	.140	3.65	-.273	52		23.4	2.301	1.065	2.16	-1.422	56
	10.3	.888	.224	3.96	-.500	55							
	11.6	1.032	.280	3.69	-.593	55	6.28	-2.0	-.079	- - -	- - -	- - -	--
	14.5	1.391	.409	3.40	-.779	54		0	0	- - -	- - -	- - -	--
	18.7	1.946	.709	2.74	-1.122	54		1.0	.038	- - -	- - -	-.020	50
								2.0	.077	- - -	- - -	-.037	44
								5.3	.299	- - -	- - -	-.169	55
4.24	-2.0	-.088	.076	-1.16	- - -	--		7.3	.470	- - -	- - -	-.276	57
	0	0	.070	0	- - -	--		9.3	.659	- - -	- - -	-.393	58
	1.0	.044	.085	.52	- - -	--		12.1	.920	- - -	- - -	-.584	59
	2.0	.087	.094	.93	- - -	--		14.1	1.151	- - -	- - -	-.705	57
	4.3	.228	.082	2.78	-.112	48		16.1	1.389	- - -	- - -	-.865	58
	7.4	.485	.124	3.91	-.262	53		19.3	1.935	- - -	- - -	- - -	--
	9.4	.700	.184	3.80	-.392	54		21.3	2.230	- - -	- - -	-.410	58
								23.3	2.529	- - -	- - -	-1.624	58

NACA

TABLE I.- EXPERIMENTAL RESULTS - Continued

M	α	C_L	C_D	$\frac{L}{D}$	C_m	$\bar{x}$	M	α	C_L	C_D	$\frac{L}{D}$	C_m	$\bar{x}$
(g) f_n = 7 cone													
3.01	-2.0	-0.062	0.059	-1.05	0.041	64	5.04	-1.0	-0.033	0.068	-0.48	- - -	--
	0	0	.053	0	0	--		0	0	.061	0	- - -	--
	1.0	.033	.062	.53	-.022	64		1.0	.035	.062	.56	- - -	--
	2.0	.065	.063	1.03	-.046	68		1.8	.051	.068	.75	-.036	68
	3.3	.112	.052	2.15	-.074	64		5.3	.180	.073	2.47	-.122	65
	4.0	.134	.063	2.13	-.091	66		7.3	.273	.095	2.87	-.185	65
	7.3	.282	.077	3.66	-.190	66		9.3	.368	.124	2.97	-.252	66
	10.2	.436	.118	3.70	-.292	65		12.1	.538	.183	2.94	-.373	66
	11.4	.544	.145	3.75	-.376	67		14.1	.658	.242	2.72	-.448	64
	14.2	.743	.228	3.38	-.503	65		16.1	.779	.311	2.50	-.530	64
	17.4	1.006	.354	2.84	-.702	66		19.3	.935	- - -	- - -	-.655	63
	18.3	1.071	.394	2.72	-.752	65		21.3	1.060	- - -	- - -	-.761	64
	21.4	1.324	.567	2.33	-.956	66		23.3	1.179	- - -	- - -	-.858	63
	25.4	1.641	.843	1.95	-1.217	66							
4.24	-2.0	-.067	.051	-1.31	.046	68	6.28	-2.0	-.045	- - -	- - -	- - -	--
	0	0	.041	0	- - -	--		0	0	.120	0	- - -	--
	1.0	.035	.053	.66	- - -	--		1.0	.024	.128	.19	- - -	--
	2.0	.065	.060	1.08	-.046	69		2.0	.051	.138	.37	- - -	--
	4.3	.131	.053	2.47	-.089	66		5.2	.171	.151	1.13	-.130	70
	7.3	.265	.074	3.58	-.180	67		7.2	.280	.167	1.68	-.200	67
	9.8	.409	.119	3.44	-.286	68		9.2	.373	.200	1.87	- - -	--
	11.1	.504	.144	3.50	-.353	66		12.1	.553	.256	1.97	-.396	67
	14.2	.691	.218	3.17	-.489	67		14.1	.664	.323	2.06	-.494	68
	16.2	.820	.289	2.84	-.594	68		16.1	.801	.408	1.96	-.575	65
	18.3	.954	.406	2.35	-.701	68		19.3	.958	- - -	- - -	-.730	66
	21.3	1.133	.546	2.08	-.841	67		21.3	1.098	.721	1.52	-.858	67
	23.9	1.287	.693	1.86	-.973	67		23.3	1.223	.853	1.43	-.959	66
(h) f_n = 7 cone, f_a = 3 cylinder													
3.01	-2.0	-.094	.079	-1.19	- - -	--	4.24	4.3	.209	.058	3.60	-.121	57
	0	0	.079	0	0	--		7.3	.424	.097	4.37	-.256	59
	1.0	.042	.083	.54	-.022	51		9.4	.607	.148	4.10	-.373	60
	2.0	.085	.080	1.06	-.046	52		11.2	.800	.221	3.62	-.517	62
	3.3	.154	.074	2.08	-.086	55		14.2	1.108	.344	3.22	-.714	62
	4.1	.182	.081	2.25	-.102	54		16.3	1.318	.453	2.91	-.863	62
	7.4	.411	.108	3.81	-.241	57							
	10.2	.701	.174	4.03	-.417	58	5.04	-2.0	-.078	.061	-1.28	- - -	--
	11.5	.859	.225	3.82	-.516	60		0	0	.058	0	- - -	--
	14.4	1.240	.374	3.32	-.769	60		1.0	.039	.062	.63	- - -	--
	18.6	1.799	.664	2.71	-1.152	60		1.8	.068	.070	.97	-.038	54
								5.3	.284	.081	3.51	- - -	--
3.49	-2.0	-.090	.075	-1.20	.050	54		7.3	.407	.118	3.45	-.248	59
	0	0	.074	0	0	--		9.3	.581	.174	3.34	-.359	60
	1.0	.052	.078	.67	-.031	57		12.1	.846	.272	3.11	-.521	59
	2.0	.091	.077	1.18	-.047	51		14.1	1.036	.357	2.90	-.633	58
	3.3	.166	.071	2.34	-.098	57		16.2	1.243	.460	2.70	-.765	58
	4.1	.189	.081	2.33	-.102	52							
	7.4	.435	.108	4.03	-.262	59	6.28	-2.0	.074	- - -	- - -	- - -	--
	10.3	.736	.179	4.11	-.451	60		0	0	.157	0	- - -	--
	11.5	.886	.231	3.84	-.556	61		1.0	.030	.139	.22	- - -	--
	14.4	1.230	.363	3.39	-.765	60		2.0	.074	.153	.48	- - -	--
	18.6	1.738	.631	2.75	-1.104	60		5.3	.252	.135	1.87	- - -	--
								7.3	.393	.225	1.75	- - -	--
4.24	-2.0	-.080	.059	-1.36	- - -	--		9.3	.594	.240	2.48	- - -	--
	0	0	.058	0	- - -	--		12.1	.866	.369	2.35	- - -	--
	1.0	.036	.063	.57	- - -	--		14.1	1.064	.464	2.29	- - -	--
	2.0	.079	.066	1.20	- - -	--		16.1	1.302	.584	2.23	- - -	--
(i) f_n = 5, 3/4 power, f_a = 2 cylinder													
3.01	-2.0	-.085	.062	-1.37	.042	48	5.04	-2.0	-.083	.058	-1.43	- - -	--
	0	0	.048	0	- - -	--		0	0	.053	0	- - -	--
	1.0	.040	.058	.69	-.019	46		1.0	.041	.052	.79	-.021	51
	2.0	.081	.068	1.19	-.041	49		1.8	.071	.055	1.29	-.038	53
	3.3	.138	.067	2.06	-.075	53		5.3	.247	.078	3.17	-.135	53
	4.0	.167	.077	2.17	-.087	50		7.3	.364	.109	3.34	-.201	54
	7.4	.373	.104	3.59	-.193	54		9.3	.503	.154	3.27	-.285	55
	10.2	.600	.167	3.59	-.335	56		12.1	.690	.236	2.92	-.406	56
	11.4	.720	.201	3.58	-.424	57		14.1	.823	.308	2.67	-.472	54
	14.3	.990	.325	3.05	-.580	56		16.1	.962	.401	2.40	-.541	52
	18.4	1.406	.559	2.52	-.858	57							

TABLE I.- EXPERIMENTAL RESULTS - Continued

M	α	C_L	C_D	$\frac{L}{D}$	C_m	x̄	M	α	C_L	C_D	$\frac{L}{D}$	C_m	x̄
(j) f_n = 5, 3/4 power, f_a = 5 cylinder													
3.01	-2.0	-0.085	0.092	-0.92	0.034	38	5.04	-2.0	-0.098	0.083	-1.18	- - -	--
	0	0	.080	0	0	--		0	0	.077	0	- - -	--
	1.0	.043	.091	.47	-.016	36		1.0	.048	.079	.61	- - -	--
	2.0	.088	.097	.91	-.035	39		1.8	.079	.081	.97	- - -	--
	3.3	.170	.093	1.83	-.077	44		5.3	.304	.102	2.98	-.155	50
	4.1	.191	.102	1.87	-.078	39		7.3	.470	.139	3.38	-.245	51
	7.4	.475	.134	3.55	-.230	47		9.3	.659	.195	3.38	-.349	51
	10.3	.800	.214	3.74	-.412	50		12.1	.943	.292	3.23	-.503	51
	11.6	1.043	.280	3.73	-.562	52		14.2	1.159	.388	2.99	-.621	51
	14.5	1.451	.432	3.36	-.788	52		16.2	1.387	.502	2.76	-.749	51
	18.7	2.110	.767	2.75	-1.183	53							
(k) f_n = 5 parabola, f_a = 2 cylinder													
3.01	-2.0	-.091	.073	-1.21	- - -	--	5.04	-2.0	-.077	.083	-.93	- - -	--
	0	0	.068	0	- - -	--		0	0	.076	0	- - -	--
	1.0	.043	.073	.59	- - -	--		1.0	.038	.078	.49	- - -	--
	2.0	.085	.080	1.06	- - -	--		1.8	.070	.085	.82	- - -	--
	3.3	.153	.075	2.04	-.078	50		5.3	.238	.104	2.29	-.121	49
	4.0	.176	.092	1.91	-.088	48		7.3	.357	.129	2.77	-.181	50
	7.4	.397	.116	3.42	-.203	50		9.3	.494	.169	2.92	-.262	51
	10.2	.624	.167	3.74	-.311	48		12.1	.688	.246	2.80	-.374	52
	11.4	.785	.222	3.54	-.424	52		14.1	.848	.319	2.66	-.450	50
	14.3	1.072	.317	3.38	-.577	52		16.1	1.020	.406	2.51	-.551	50
	18.4	1.531	.547	2.80	-.854	53							
(l) f_n = 5 parabola, f_a = 5 cylinder													
3.01	-2.0	-.090	.094	-.96	.033	35	5.04	-2.0	- - -	.082	- - -	- - -	--
	0	0	.083	0	- - -	--		0	- - -	.080	- - -	- - -	--
	1.0	.042	.091	.46	-.015	35		1.0	- - -	.083	- - -	- - -	--
	2.0	.088	.099	.89	-.033	36		1.8	- - -	.086	- - -	- - -	--
	3.3	.164	.092	1.78	-.060	35		5.3	.311	.130	2.39	-.142	44
	4.1	.193	.112	1.72	-.070	35		7.3	.486	.172	2.83	-.237	47
	7.4	.485	.148	3.28	-.208	41		9.3	.684	.230	2.97	-.346	48
	10.4	.839	.238	3.53	-.392	45		12.2	.971	.361	2.69	-.489	48
	11.6	1.105	.310	3.57	-.563	49		14.2	1.201	.462	2.60	-.611	48
	14.7	1.520	.446	3.41	-.771	49		16.2	1.447	.585	2.47	-.759	49
	18.8	2.224	.724	3.07	-1.155	50							
(m) f_n = 5 ogive, f_a = 2 cylinder													
3.01	-2.0	-.088	.079	-1.11	.038	41	5.04	-2.0	-.092	.080	-1.15	- - -	--
	0	0	.071	0	- - -	--		0	0	.076	0	- - -	--
	1.0	.048	.077	.62	- - -	--		1.0	.043	.079	.54	- - -	--
	2.0	.092	.075	1.23	-.039	41		1.8	.079	.071	1.11	- - -	--
	3.3	.169	.082	2.06	-.074	43		5.3	.271	.094	2.88	-.143	52
	4.1	.192	.092	2.09	-.086	43		7.3	.394	.126	3.14	-.211	52
	7.4	.429	.126	3.41	-.212	48		9.3	.532	.171	3.11	-.284	51
	10.2	.676	.185	3.65	-.344	49		12.1	.748	.282	2.65	-.404	51
	11.5	.815	.235	3.47	-.434	51		14.1	.902	.350	2.58	-.492	51
	14.3	1.127	.342	3.30	-.606	52		16.1	1.068	.435	2.45	-.600	52
	18.5	1.577	.559	2.82	-.882	53							
(n) f_n = 5 ogive, f_a = 5 cylinder													
3.01	-2.0	-.099	.101	-.98	.030	29	5.04	-2.0	-.105	.089	-1.18	- - -	--
	0	0	.094	0	- - -	--		0	0	.082	0	- - -	--
	1.0	.048	.104	.46	-.014	29		1.0	.051	.082	.62	- - -	--
	2.0	.097	.105	.92	-.023	22		1.8	.089	.085	1.05	- - -	--
	3.3	.181	.107	1.69	-.061	32		5.3	.343	.123	2.79	-.160	45
	4.1	.207	.110	1.87	-.058	28		7.3	.516	.161	3.21	-.249	47
	7.5	.514	.156	3.29	-.211	40		9.3	.710	.212	3.35	-.349	48
	10.4	.899	.244	3.68	-.439	47		12.1	.994	.345	2.88	-.508	51
	11.7	1.140	.318	3.59	-.578	49		14.2	1.218	.437	2.79	-.647	50
	14.6	1.562	.475	3.29	-.808	50		16.2	1.477	.564	2.62	-.801	51
	18.8	2.248	.817	2.75	-1.212	51							

TABLE I.- EXPERIMENTAL RESULTS - Concluded

M	α	C_L	C_D	$\frac{L}{D}$	C_m	$\bar{x}$	M	α	C_L	C_D	$\frac{L}{D}$	C_m	$\bar{x}$
(o) Flat-bottom body, $f_n = 3$, $f_a = 7$													
3.01	-2.2	-0.340	0.255	-1.33	0.037	11	4.24	9.4	0.693	0.239	2.90	-0.429	59
	-.1	-.172	.230	-.75	-.021	-12		12.3	1.096	.351	3.12	-.664	58
	.9	-.098	.221	-.44	-.044	-47		14.3	1.392	.451	3.07	-.831	57
	2.0	-.023	.219	-.10	-.075	-469		16.4	1.720	.602	2.86	-1.021	56
	3.3	.070	.204	.34	-.092	113		21.6	2.633	1.064	2.48	-1.536	54
	4.0	.136	.215	.63	-.131	87							
	7.4	.506	.239	2.11	-.302	57	6.28	-2.0	-.504	.337	-1.50	.070	14
	10.4	.949	.325	2.92	-.552	56		0	-.330	.298	-1.11	-.046	-14
	11.7	1.139	.381	2.99	-.657	55		1.0	-.290	.244	-1.19	-.067	-23
	14.6	1.658	.542	3.06	-.961	55		2.0	-.230	.248	-.93	-.051	-23
	18.9	2.446	.913	2.68	-1.428	55		5.3	.111	.211	.53	-.116	89
								7.3	.330	.228	1.45	-.256	72
4.24	-2.1	-.368	.248	-1.49	.055	15		9.3	.574	.272	2.11	-.408	67
	-.1	-.212	.218	-.97	-.005	-2		12.1	.930	.384	2.42	-.555	56
	.9	-.125	.211	-.59	-.043	-35		14.1	1.207	.478	2.53	-.718	56
	2.0	-.067	.204	-.33	-.072	-120		16.1	1.526	.617	2.47	-.843	52
	4.3	.140	.169	.83	-.150	99		19.3	2.056	.965	2.13	-1.195	53
	7.3	.444	.191	2.33	-.293	63		23.4	2.809	1.422	1.98	-1.612	51
(p) Flat-bottom body, $f_n = 5$, $f_a = 5$													
3.01	-7.6	-.734	.237	-3.10	.313	41	4.24	2.0	.002	.115	.02	-.051	1012
	-4.2	-.397	.159	-2.50	.140	34		2.1	.033	.085	.39	-.038	106
	-2.1	-.243	.155	-1.57	.084	34		4.3	.152	.085	1.79	-.122	77
	-1.1	-.152	.128	-1.19	.021	14		7.3	.407	.139	2.93	-.275	65
	-.1	-.088	.141	-.62	.010	11		9.4	.590	.175	3.37	-.386	63
	0	-.071	.124	-.57	-.021	-30		11.2	.845	.229	3.69	-.549	63
	1.0	-.018	.146	-.12	-.041	-257		14.3	1.231	.349	3.53	-.781	61
	2.0	.045	.126	.36	-.071	143		16.3	1.522	.464	3.28	-.974	61
	3.3	.124	.125	.99	-.107	81		18.5	1.847	.643	2.87	-1.183	61
	4.1	.173	.133	1.30	-.133	73		21.5	2.326	.930	2.50	-1.511	60
	7.4	.456	.164	2.78	-.298	63		23.6	2.640	1.156	2.28	-1.729	60
	10.3	.805	.222	3.63	-.505	61							
	11.6	.946	.266	3.56	-.610	62	6.28	-2.0	-.319	.256	-1.25	-.220	67
	14.5	1.416	.399	3.55	-.897	61		0	-.201	.213	-.94	-.188	94
	18.8	2.117	.715	2.96	-1.328	59		1.0	-.141	.194	-.73	-.014	10
4.24	-9.5	-.862	.307	-2.81	.404	45		2.0	-.075	.173	-.43	.026	-37
	-7.4	-.714	.233	-3.06	.332	45		5.3	.096	.143	.67	.103	96
	-4.4	-.446	.155	-2.88	.181	40		7.3	.299	.174	1.72	.224	70
	-2.2	-.281	.131	-2.15	.079	28		9.3	.477	.214	2.23	.316	63
	-2.0	-.246	.116	-2.12	.085	34		12.1	.885	.325	2.72	.602	64
	-1.0	-.172	.099	-1.74	.044	25		14.1	1.154	.436	2.65	.764	62
	0	-.132	.114	-1.16	.029	2		16.1	1.452	.569	2.55	.935	60
	.1	-.100	.093	-1.08	.007	7		19.3	1.855	.811	2.29	1.155	57
	1.0	-.060	.113	-.53	-.031	-53		21.3	2.098	.961	2.18	1.274	55
								23.3	2.445	1.189	2.06	1.508	55
(q) Flat-bottom body, $f_n = 7$, $f_a = 3$													
3.01	-2.1	-.209	.106	-1.97	.085	40	4.24	11.2	.685	.172	3.98	-.486	69
	0	-.075	.096	-.78	.006	8		14.2	1.021	.276	3.70	-.705	67
	1.0	-.012	.096	-.12	-.029	-294		16.2	1.274	.377	3.38	-.871	66
	2.0	.043	.099	.43	-.061	133		21.5	2.038	.773	2.64	-1.421	65
	3.3	.113	.088	1.28	-.106	90		23.5	2.328	.996	2.34	-1.637	65
	4.0	.149	.107	1.39	-.127	82							
	7.4	.377	.115	3.28	-.270	70	6.28	-2.0	-.281	.134	-2.10	.139	49
	10.2	.648	.173	3.75	-.444	67		0	-.152	.108	-1.41	.036	24
	11.5	.756	.198	3.82	-.516	66		1.0	-.113	- - -	- - -	- - -	- -
	14.4	1.133	.301	3.76	-.766	65		2.0	-.077	- - -	- - -	- - -	- -
	18.6	1.780	.566	3.15	-1.205	65		5.2	.080	.085	.94	- - -	- -
								7.2	.228	.108	2.11	-.149	62
4.24	-2.1	-.231	.091	-2.54	.100	43		9.3	.383	.139	2.75	-.256	64
	0	-.102	.079	-1.29	.023	22		12.1	.715	- - -	- - -	-.511	67
	1.0	-.044	.081	-.54	-.009	-22		14.1	.961	.384	2.50	-.672	66
	2.0	.002	.086	0	-.039	786		16.1	1.213	.510	2.38	-.838	64
	4.3	.131	.075	1.75	-.117	86		19.3	1.703	.723	2.36	-1.170	63
	7.3	.318	.095	3.35	-.235	72		23.3	2.292	1.090	2.10	-1.608	63
	9.3	.478	.125	3.82	-.333	68							

NACA

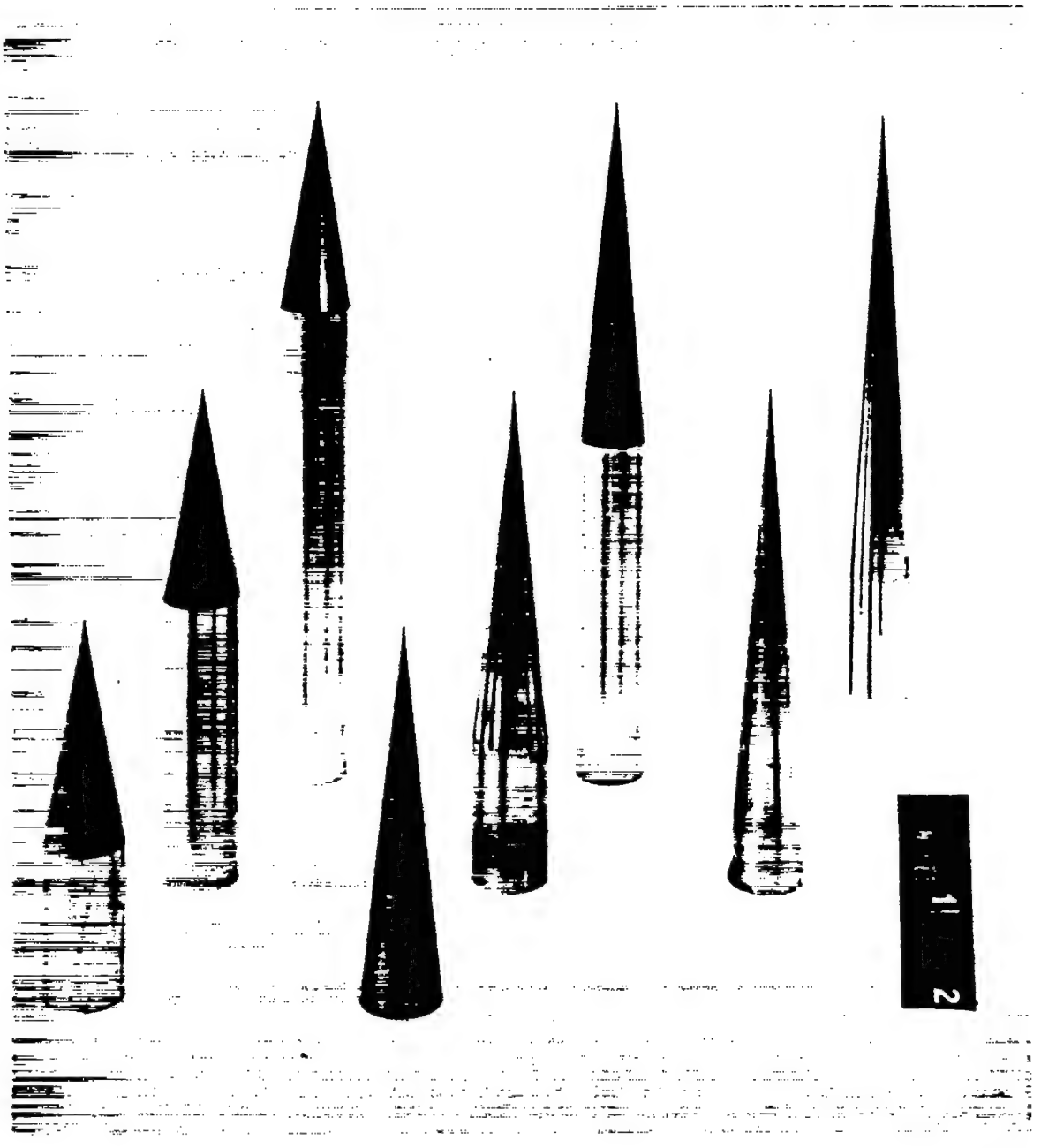

A-18936

$f_n = 3$ $f_n = 5$ $f_n = 7$

(a) Cone-cylinder bodies of fineness ratios 5, 7, and 10.

Figure 1.- Test bodies.

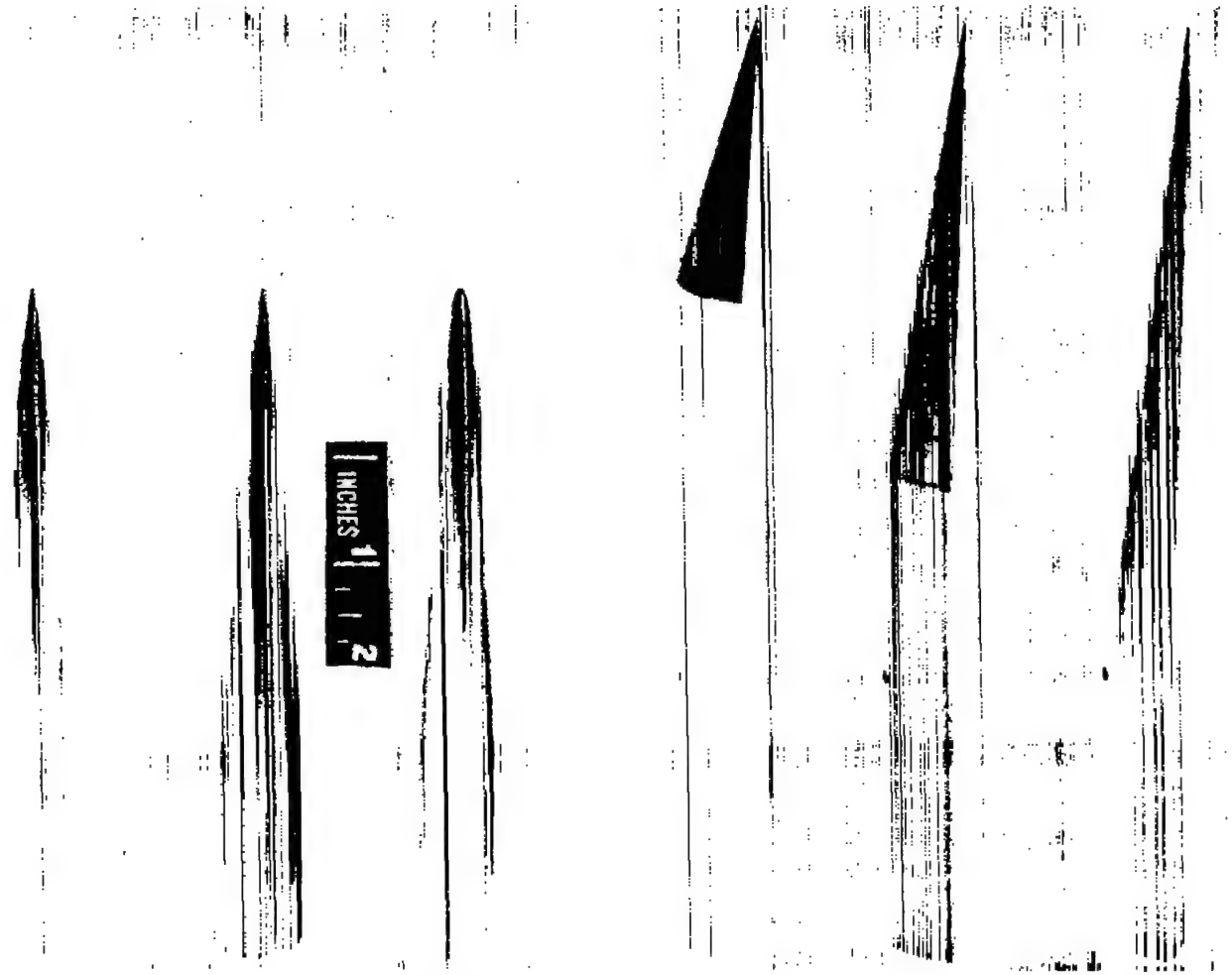

Ogive 3/4 power Parabola $f_n = 3$ $f_n = 5$ $f_n = 7$

(b) Fineness ratio 7 nose cylinder bodies ($f_n = 5$). (c) Fineness ratio 10 flat-bottom bodies

Figure 1.- Continued.

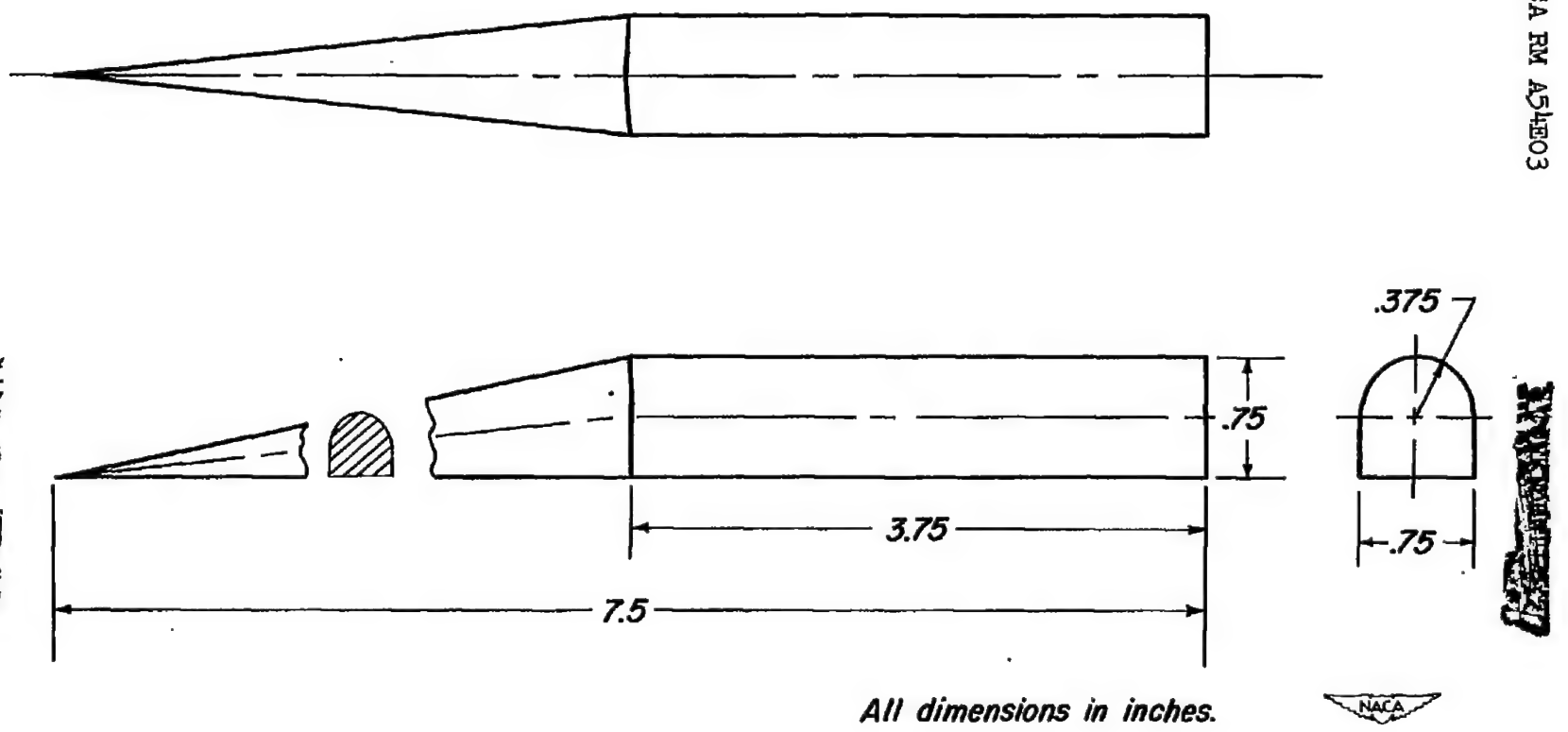

(d) Sketch of typical modified cone-cylinder flat-bottom body; ($f_n = 5$, $f_a = 5$)

Figure 1.– Concluded.

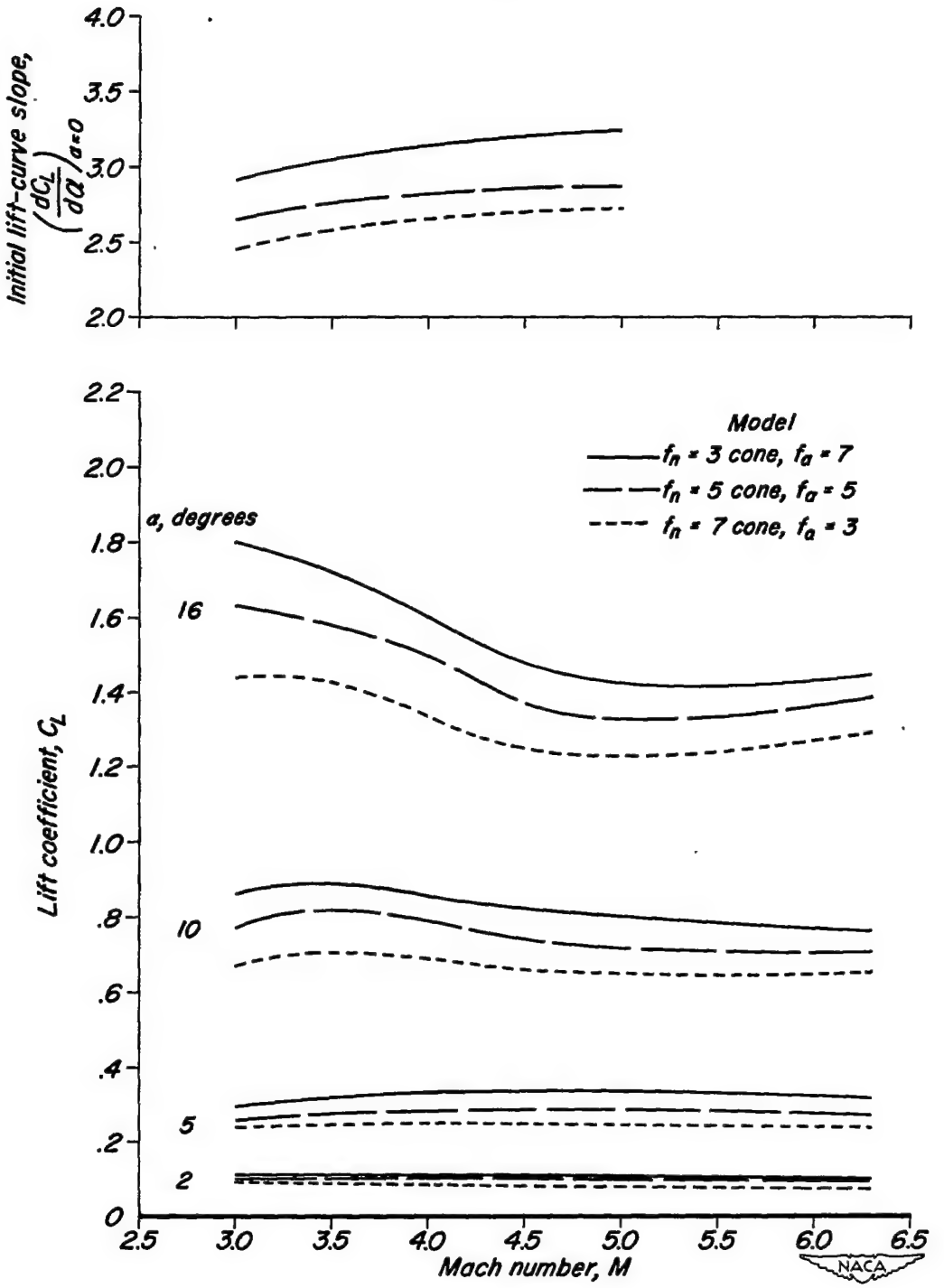

Figure 2.– Variations with Mach number of initial lift-curve slopes and of lift coefficients at several angles of attack for three fineness ratio 10 cone-cylinder bodies of revolution.

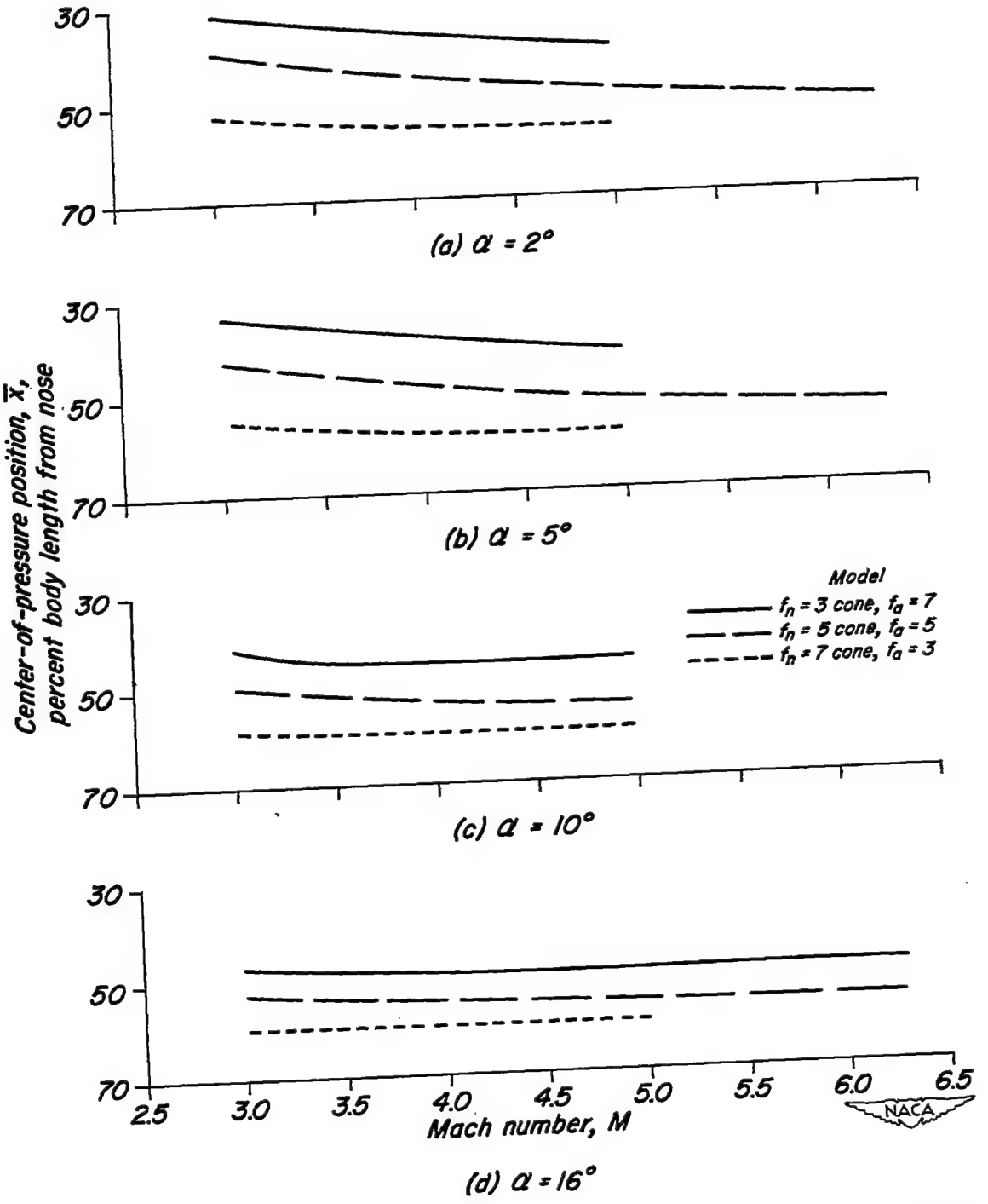

Figure 3.– Variations with Mach number of the center-of-pressure positions for three fineness ratio 10 cone-cylinder bodies of revolution at several angles of attack.

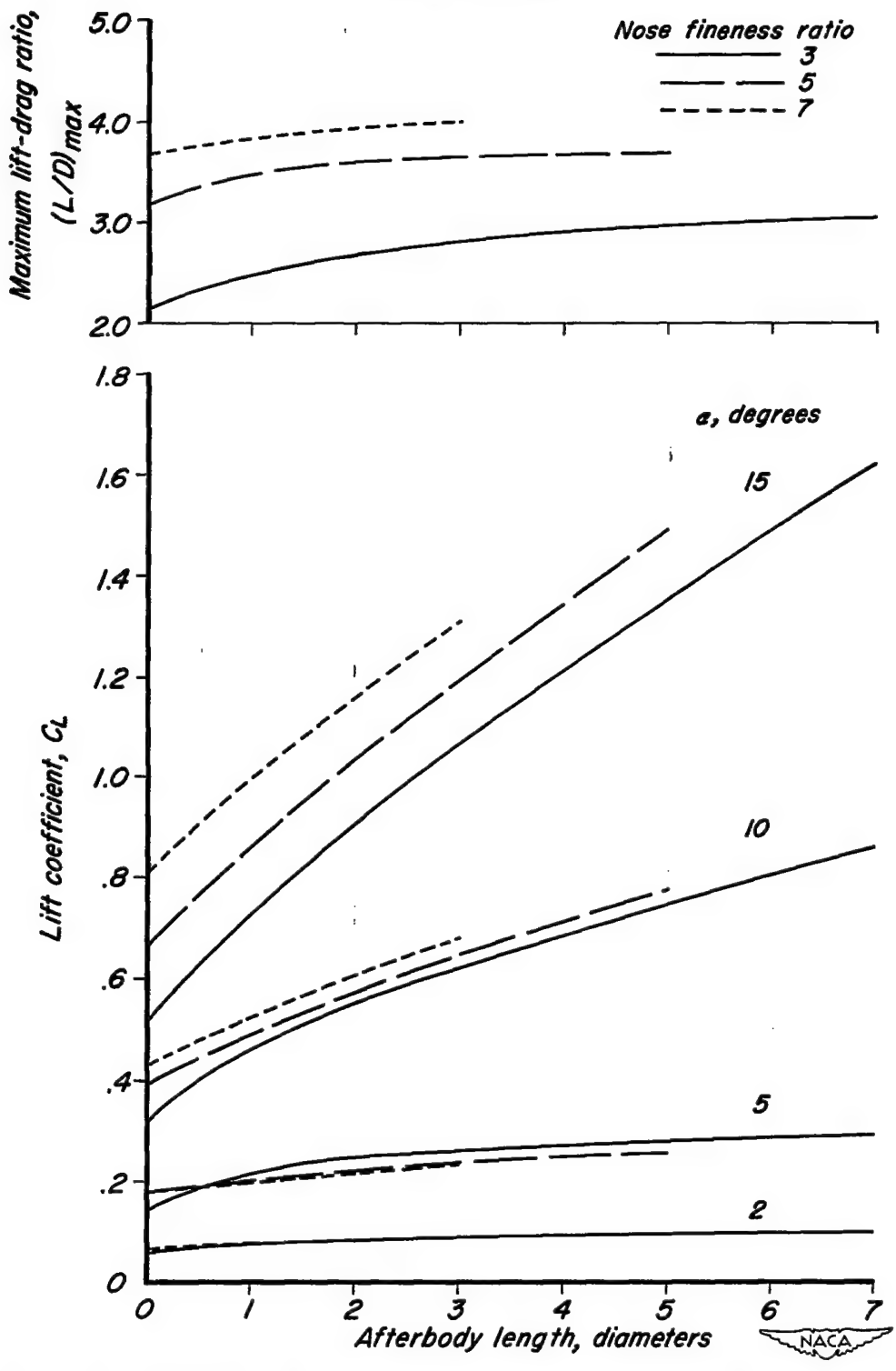

Figure 4.- Variations of maximum lift-drag ratios and of lift coefficients at several angles of attack with cylindrical afterbody length for cone-cylinder bodies of revolution at Mach number 3.0.

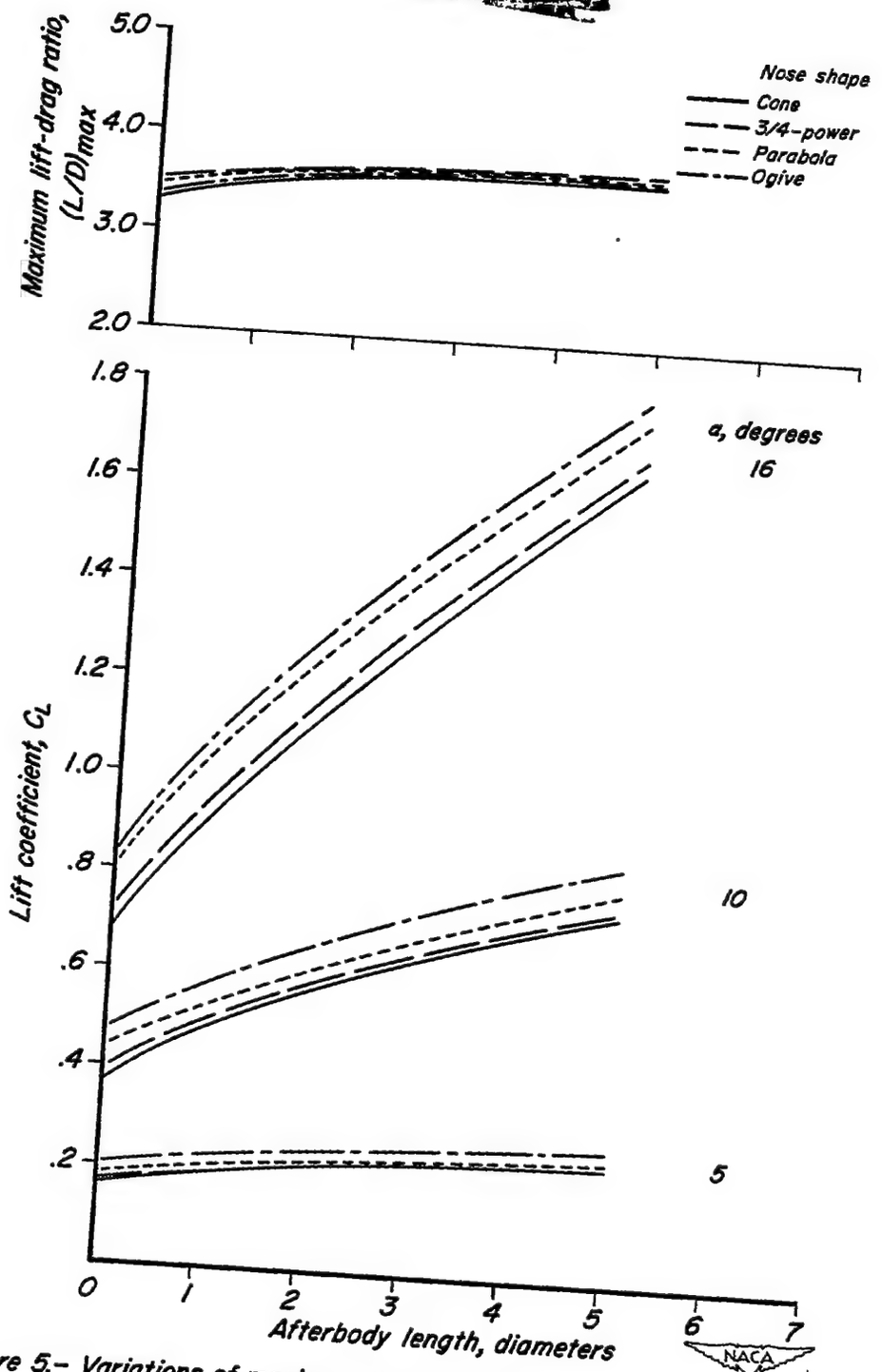

Figure 5.- Variations of maximum lift-drag ratios and of lift coefficients at several angles of attack with cylindrical afterbody length for bodies of revolution having 5 diameter long noses of different profile shapes at Mach number 3.0.

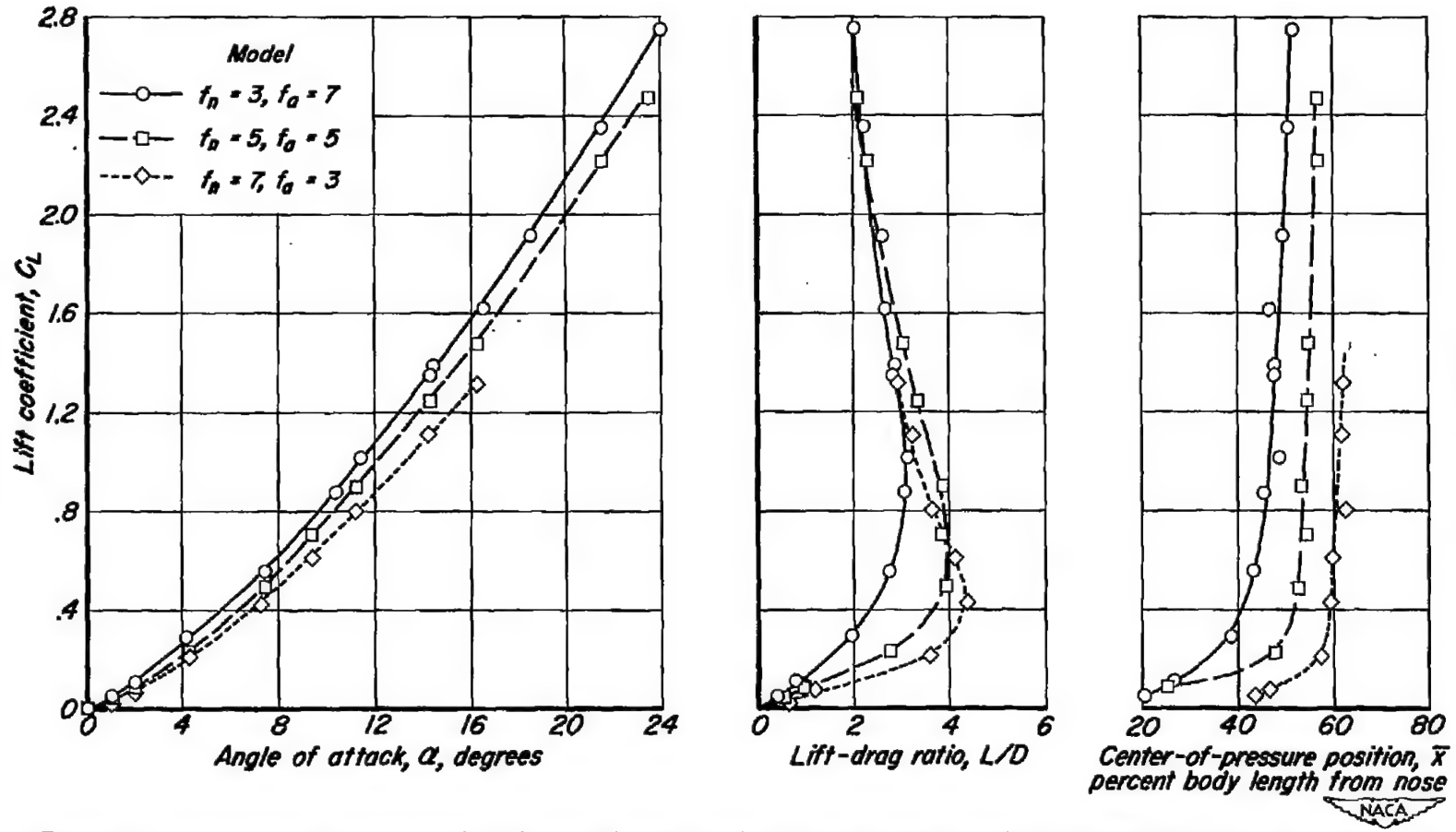

Figure 6.- Aerodynamic characteristics of three fineness ratio 10 cone-cylinder bodies of revolution at Mach number 4.2.

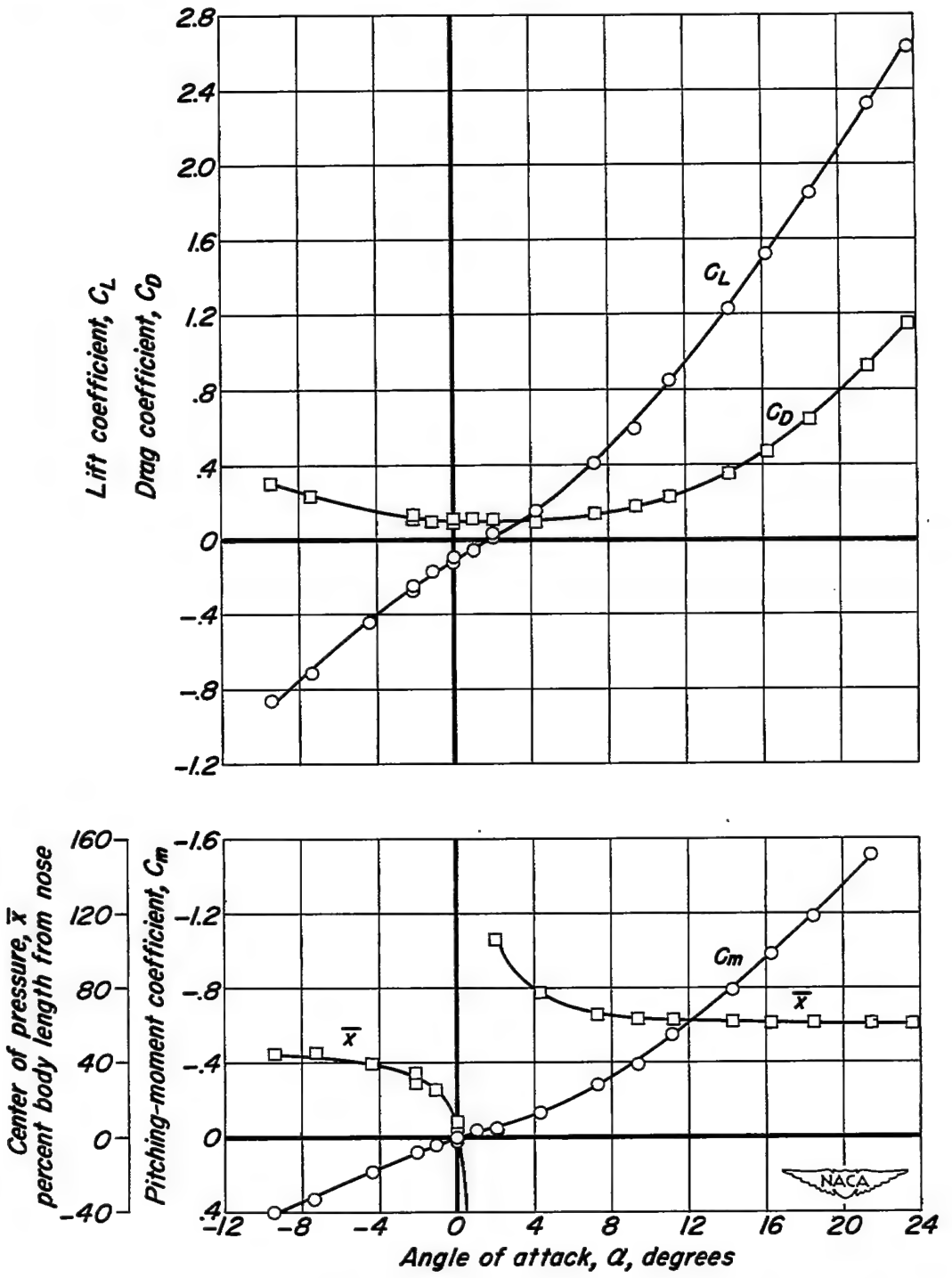

Figure 7.– Aerodynamic characteristics at Mach number 4.2 of a cone-cylinder flat-bottom body having a fineness ratio 5 nose and fineness ratio 5 afterbody.

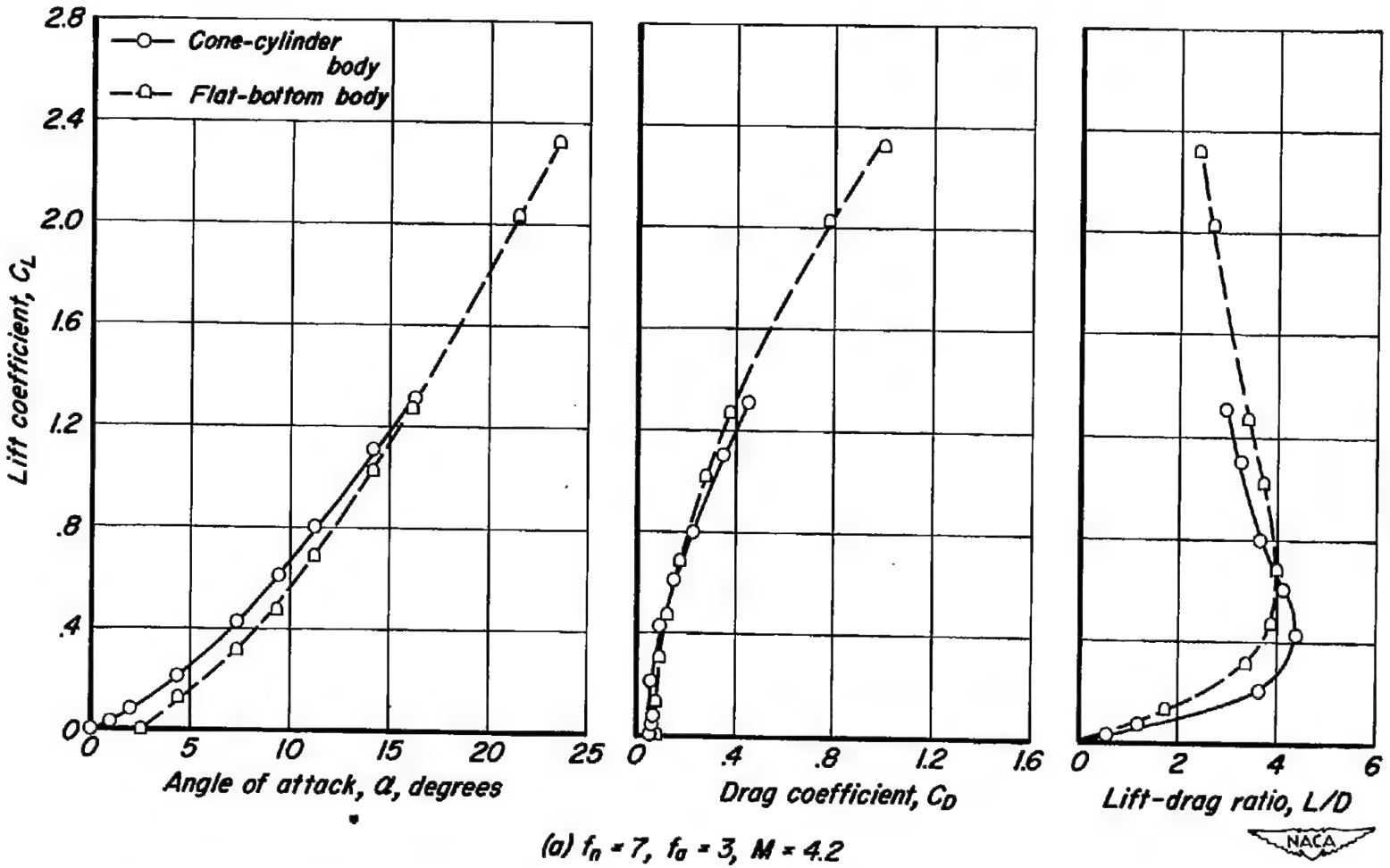

(a) $f_n = 7$, $f_a = 3$, $M = 4.2$

Figure 8.- Comparisons of the force characteristics of fineness ratio 10 cone-cylinder bodies with those of cone-cylinder flat-bottom bodies having the same nose and afterbody fineness ratios.

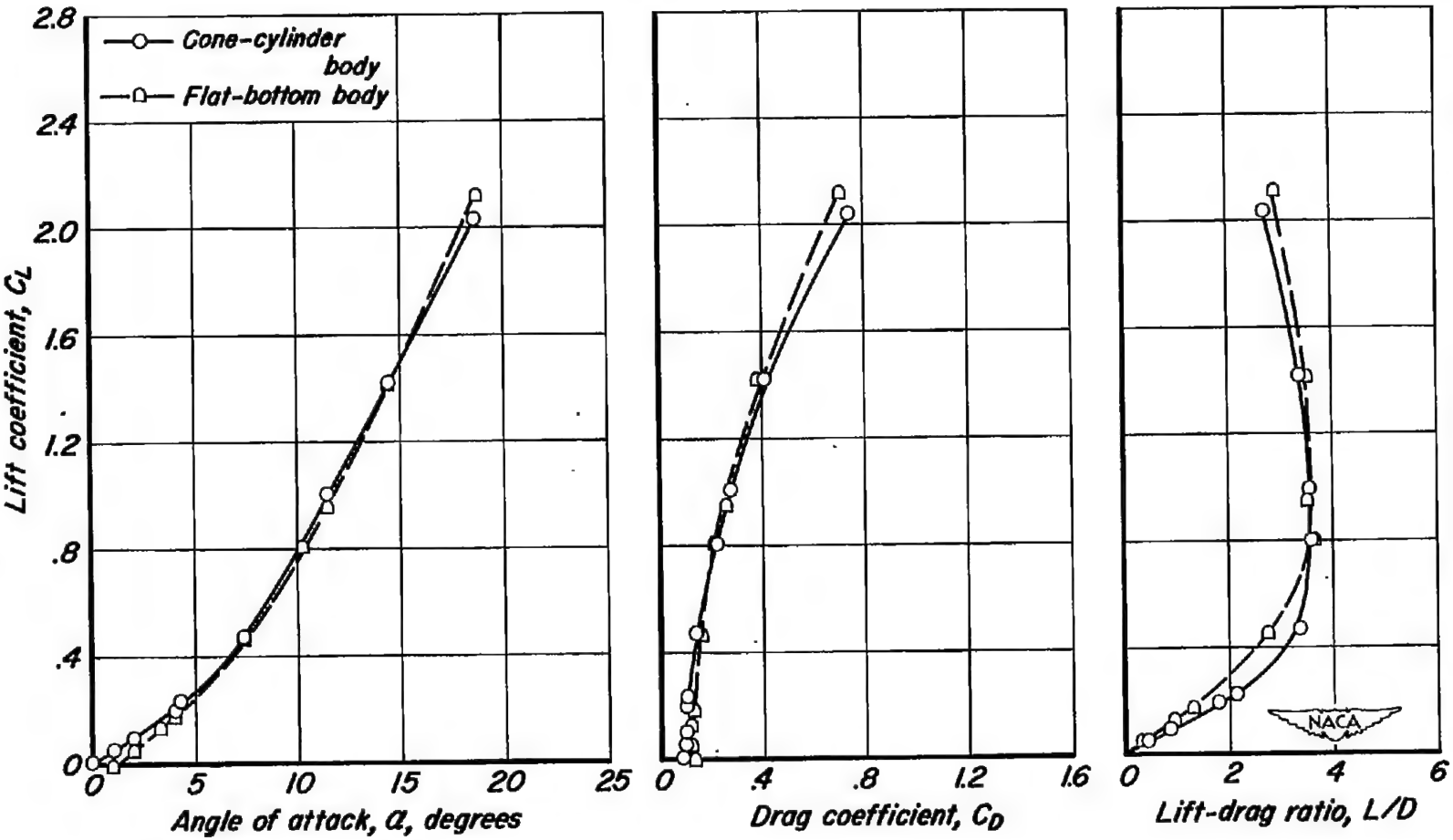

(b) $f_n = 5$, $f_a = 5$, $M = 3.0$

Figure 8.- Continued.

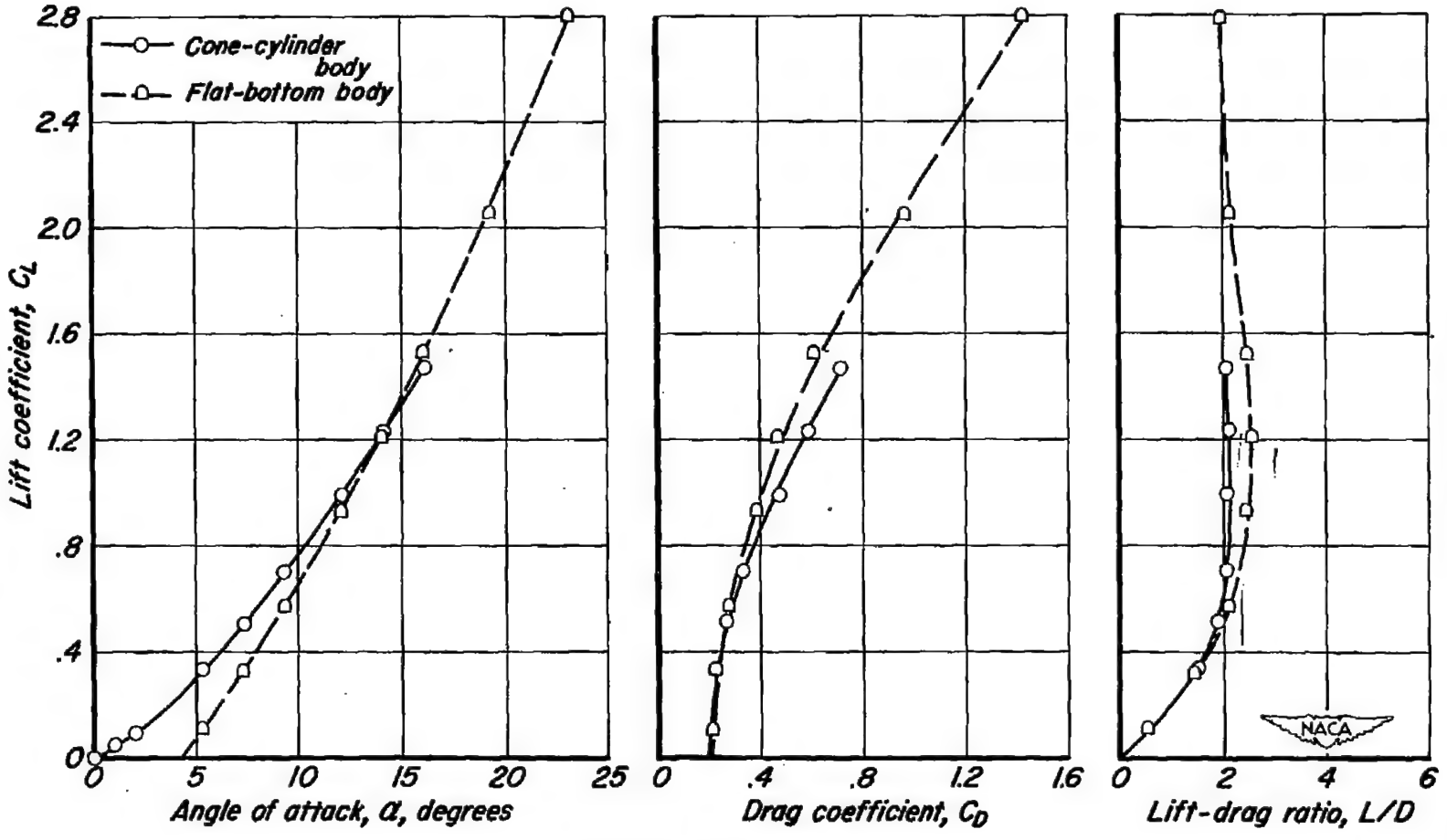

(c) $f_n = 3$, $f_a = 7$, $M = 6.3$

Figure 8.– Concluded.

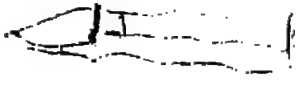

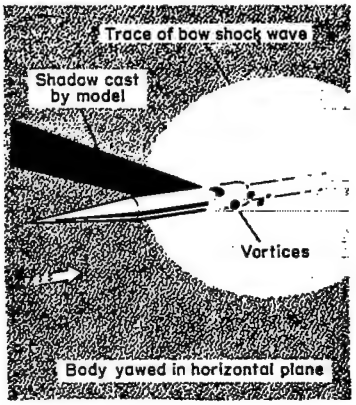

(a) Sketch of typical vapor-screen photograph

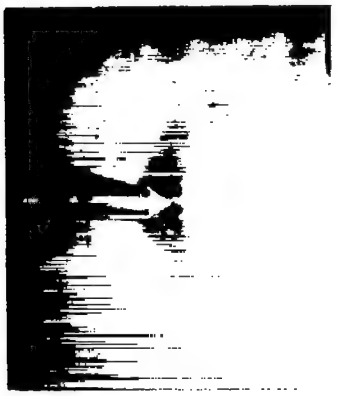

(b) $f_n = 3$, $f_a = 7$, $M = 3.5$, $\alpha = 15^\circ$

(c) $f_n = 3$, $f_a = 7$, $M = 3.5$, $\alpha = 25^\circ$

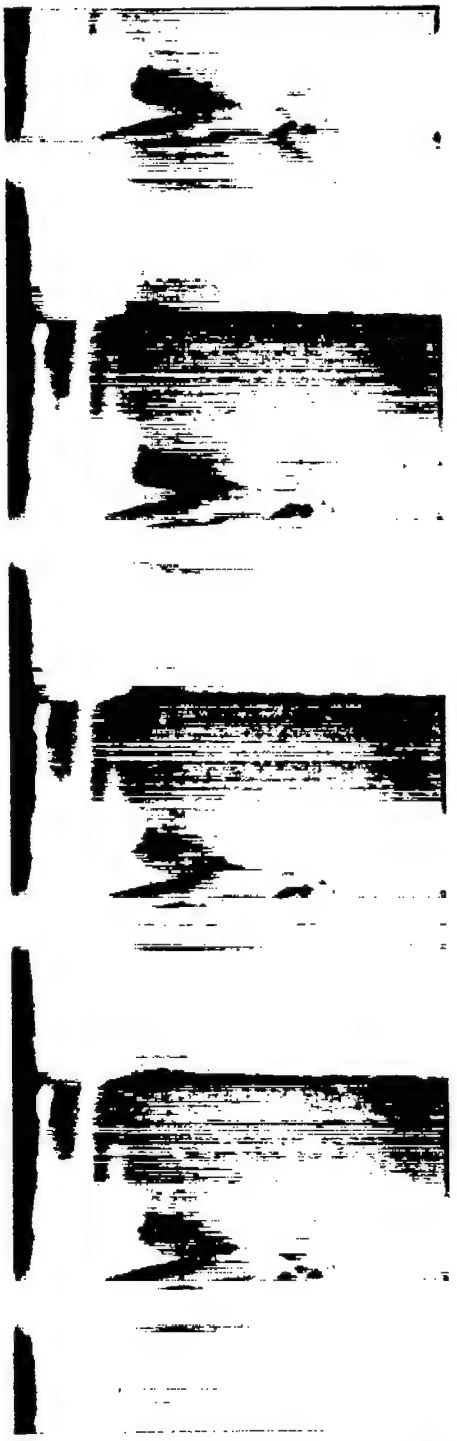

A-19072

(d) $f_n = 7$, $f_a = 3$, $M = 4.2$, $\alpha = 20^\circ$

Figure 9.- Vapor-screen photographs of the flow about two fineness ratio 10 cone-cylinder bodies.

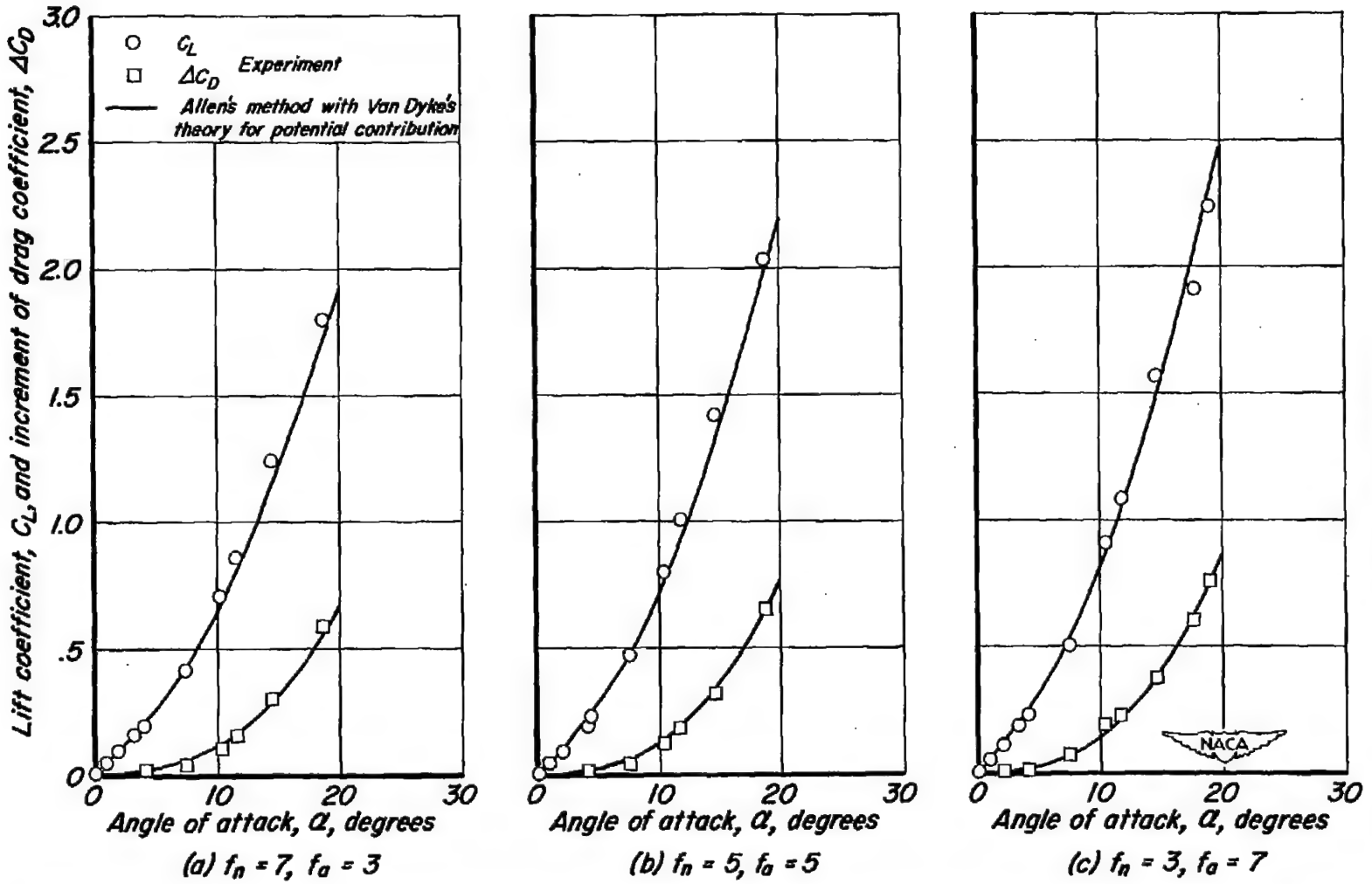

Figure 10.– Comparison of experimental force characteristics of fineness ratio 10 cone-cylinder bodies at Mach number 3.0 with those predicted with Allen's crossflow method (Van Dyke's theory used for inviscid-flow contribution).

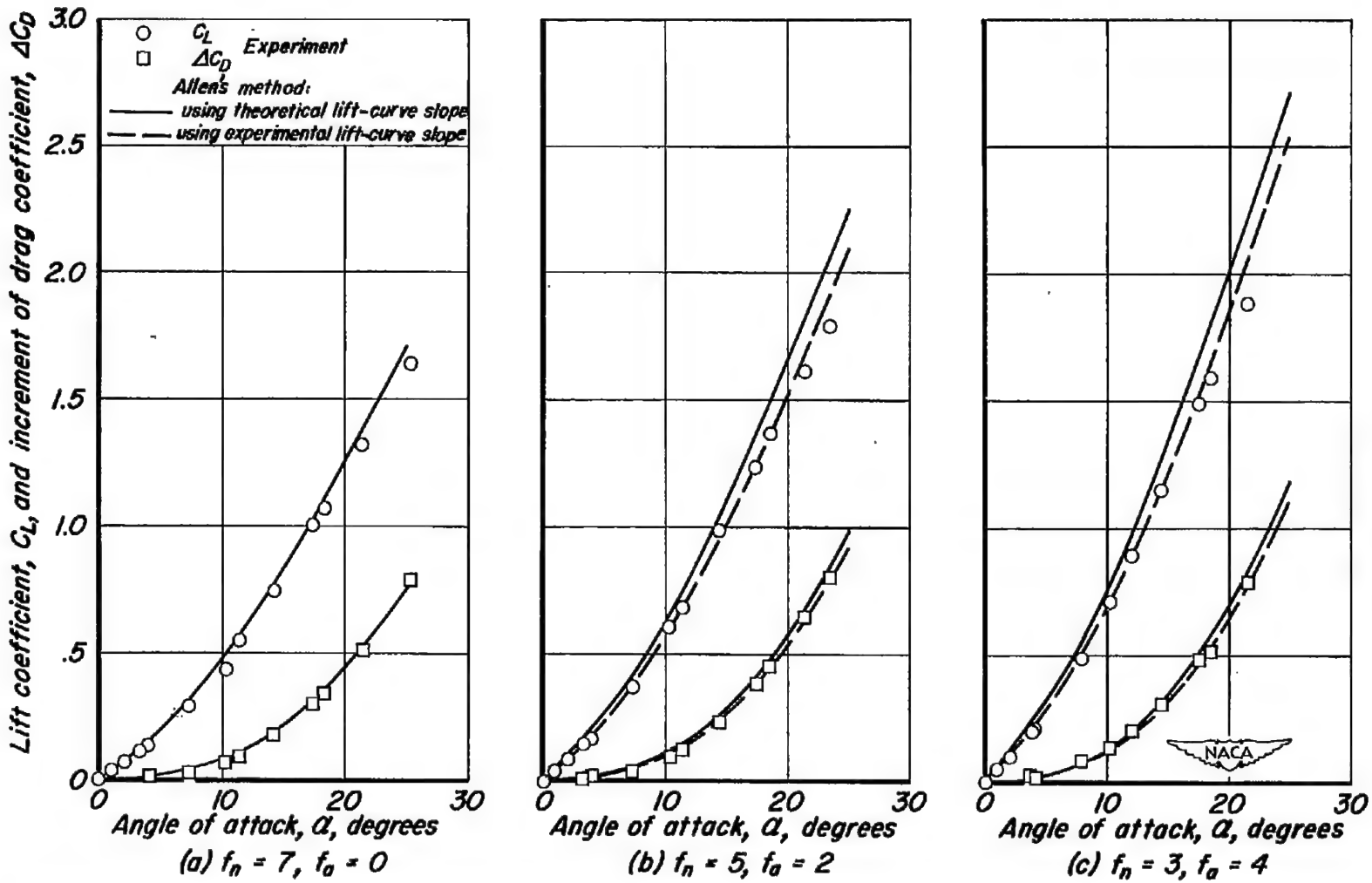

Figure 11.– Comparisons of experimental force characteristics of fineness ratio 7 cone-cylinder bodies at Mach number 3.0 with those predicted with Allen's crossflow method (Van Dyke's theory or experimental inital lift-curve slopes used for inviscid-flow contribution).

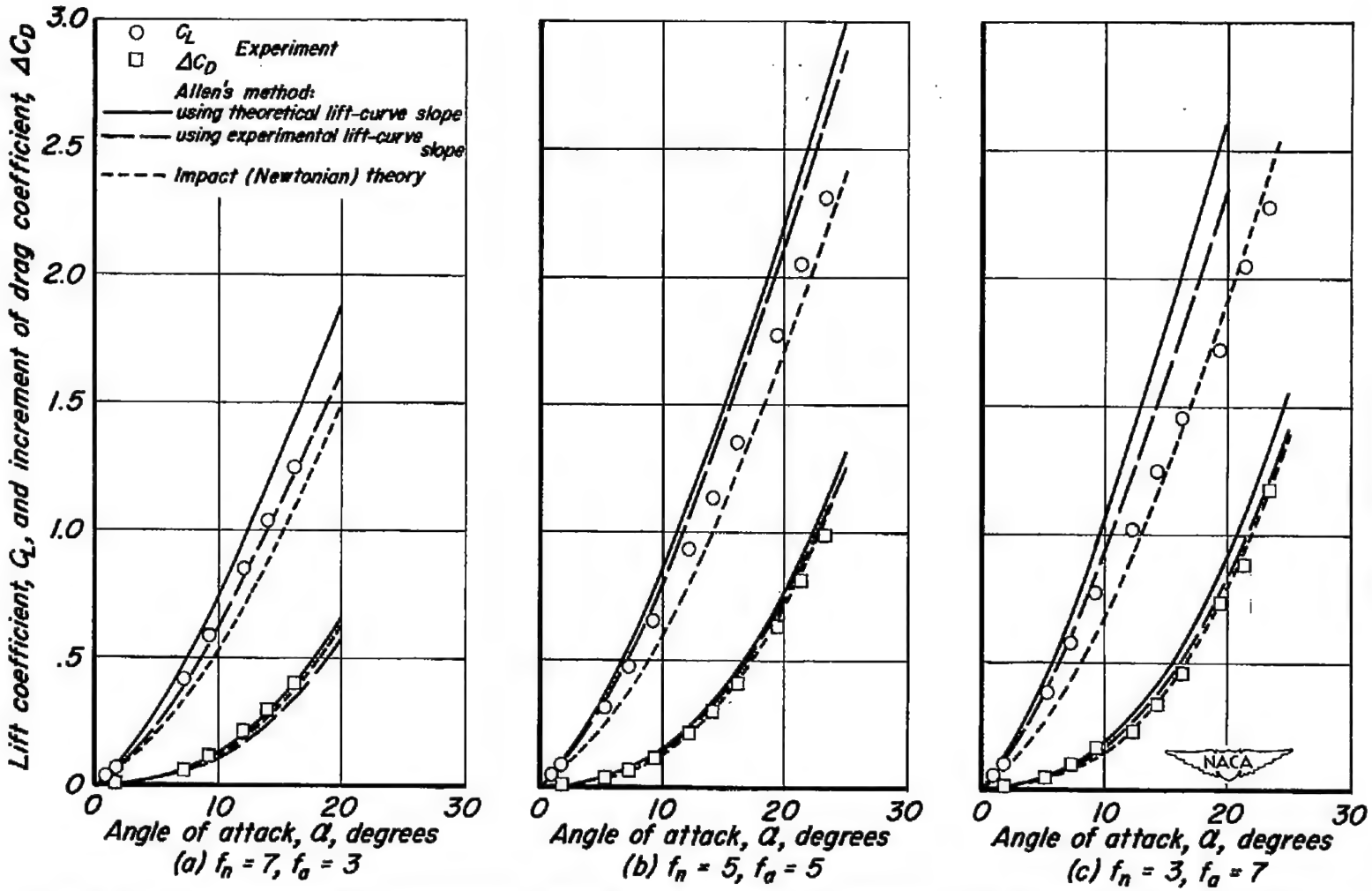

Figure 12.– Comparisons of experimental force characteristics of fineness ratio 10 cone-cylinder bodies at Mach number 5.0 with those predicted with impact theory and with Allen's crossflow method (Van Dyke's theory or experimental inital lift-curve slopes used for inviscid-flow contribution).

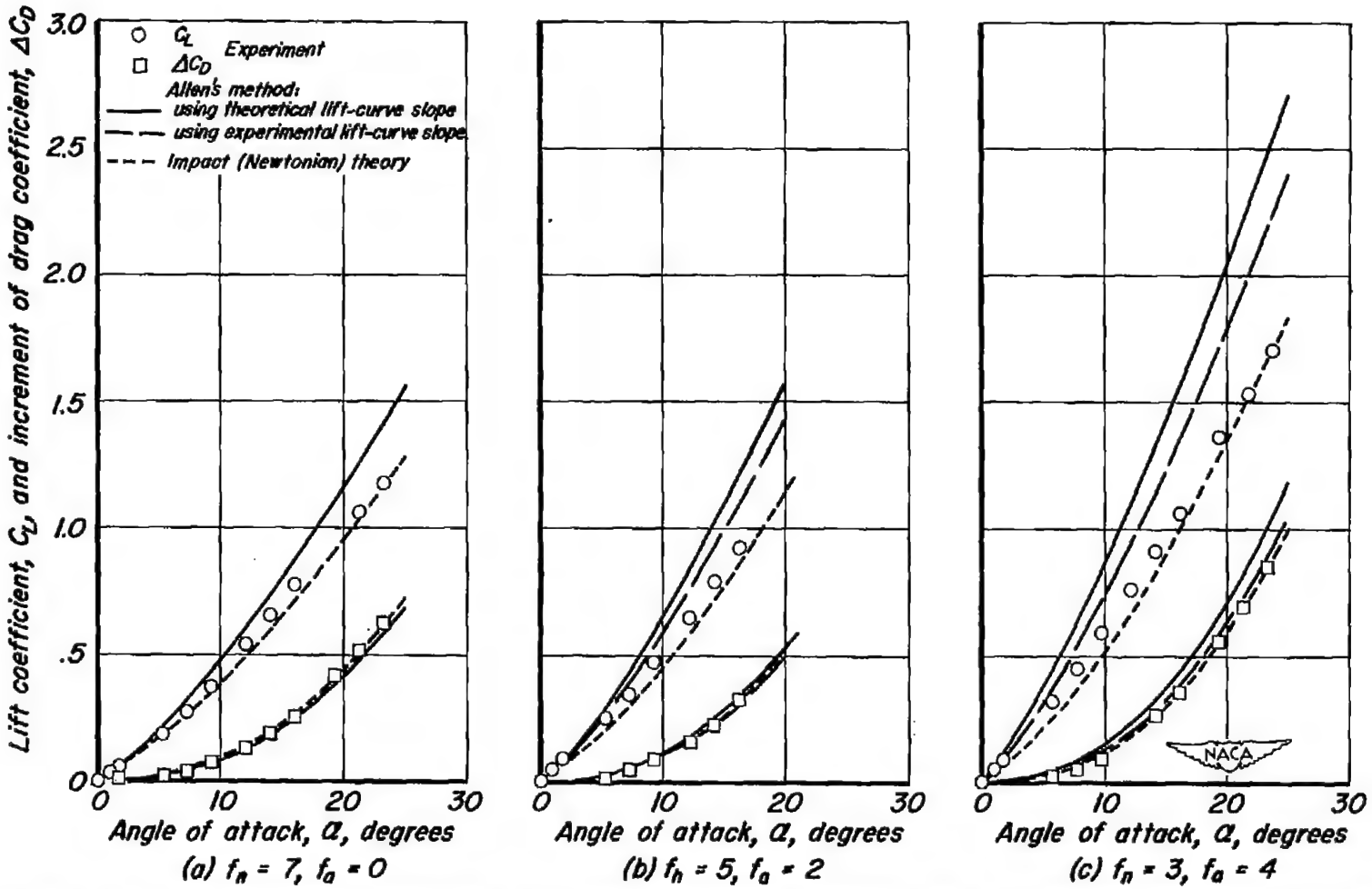

Figure 13.– Comparisons of experimental force characteristics of fineness ratio 7 cone-cylinder bodies at Mach number 5.0 with those predicted with impact theory and with Allen's crossflow method (Van Dyke's theory or experimental inital lift-curve slopes used for inviscid-flow contribution).

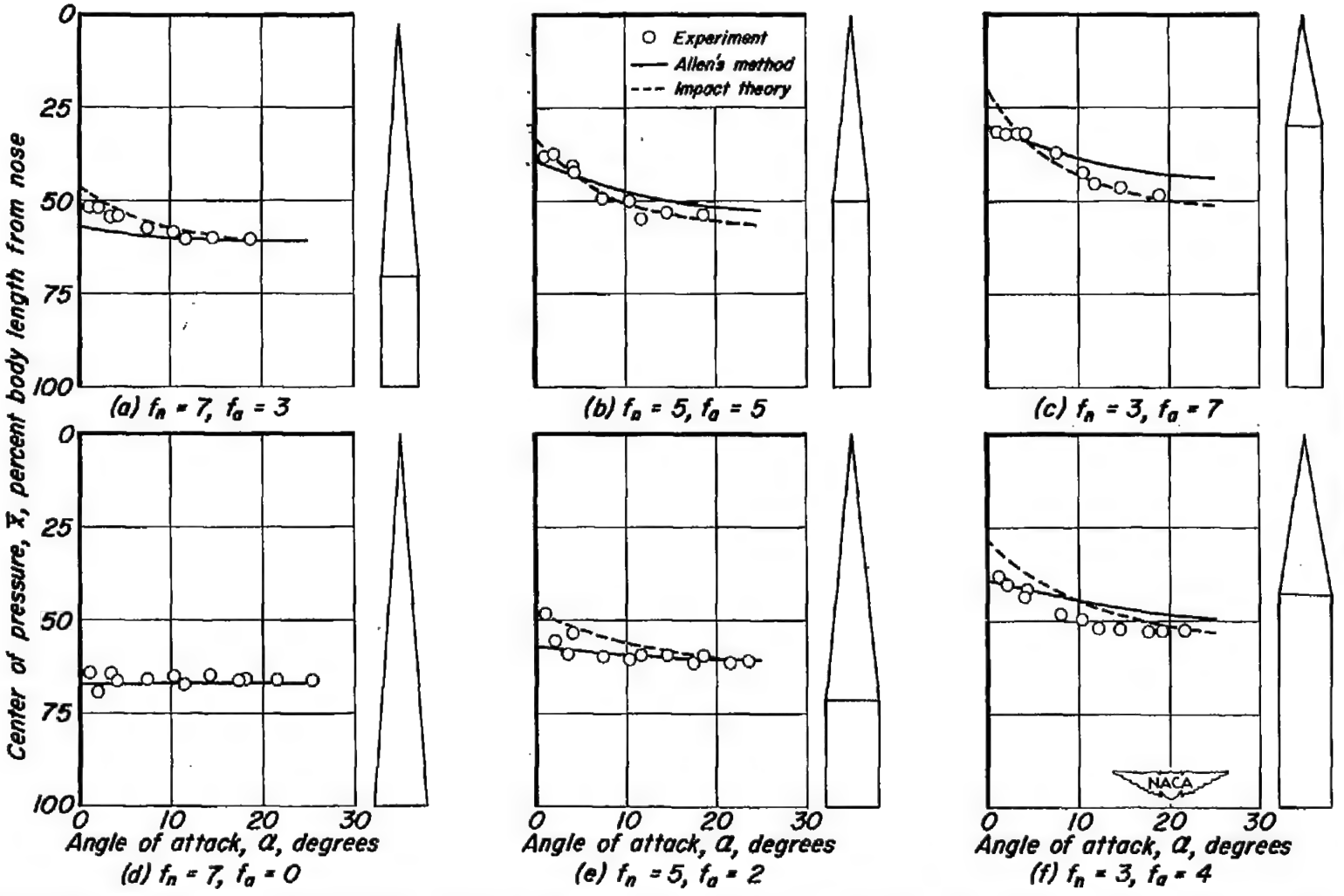

Figure 14.– Comparison of theoretical and experimental center-of-pressure positions for fineness ratio 10 and 7 cone-cylinder bodies at Mach number 3.0.

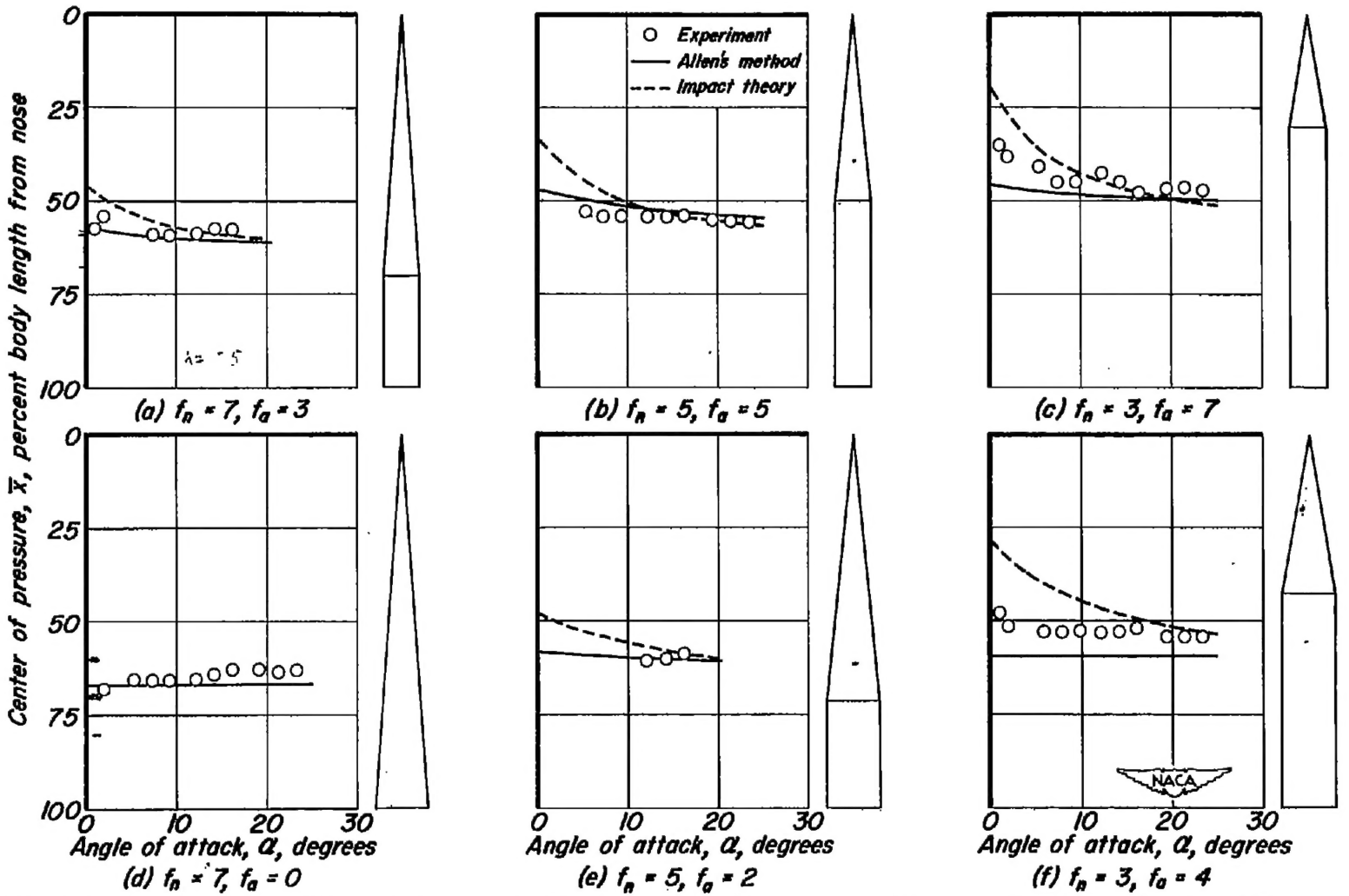

Figure 15.– Comparison of theoretical and experimental center-of-pressure positions for fineness ratio 10 and 7 cone-cylinder bodies at Mach number 5.0.

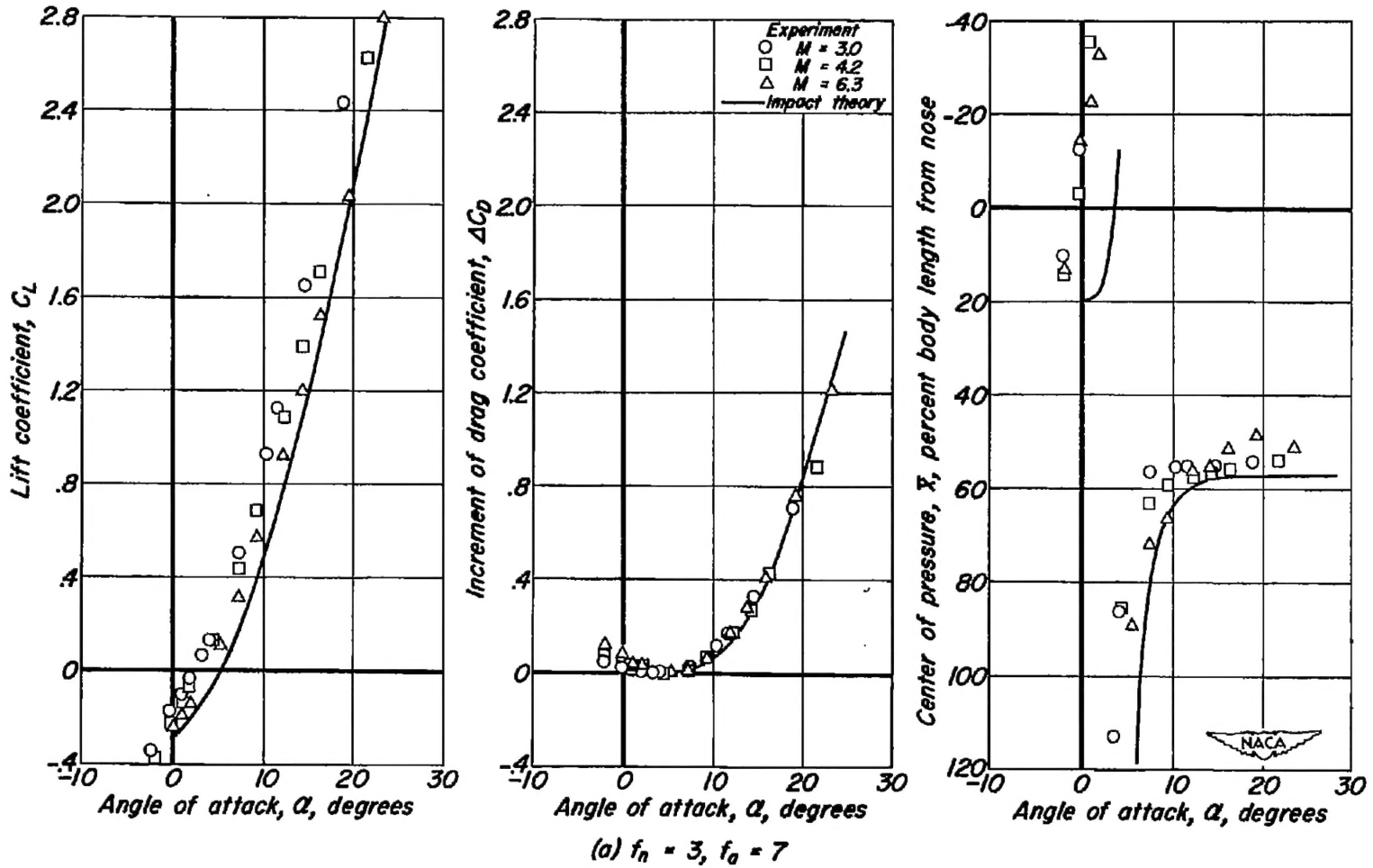

Figure 16.– Comparison of theoretical and experimental aerodynamic characteristics of cone-cylinder flat-bottom bodies.

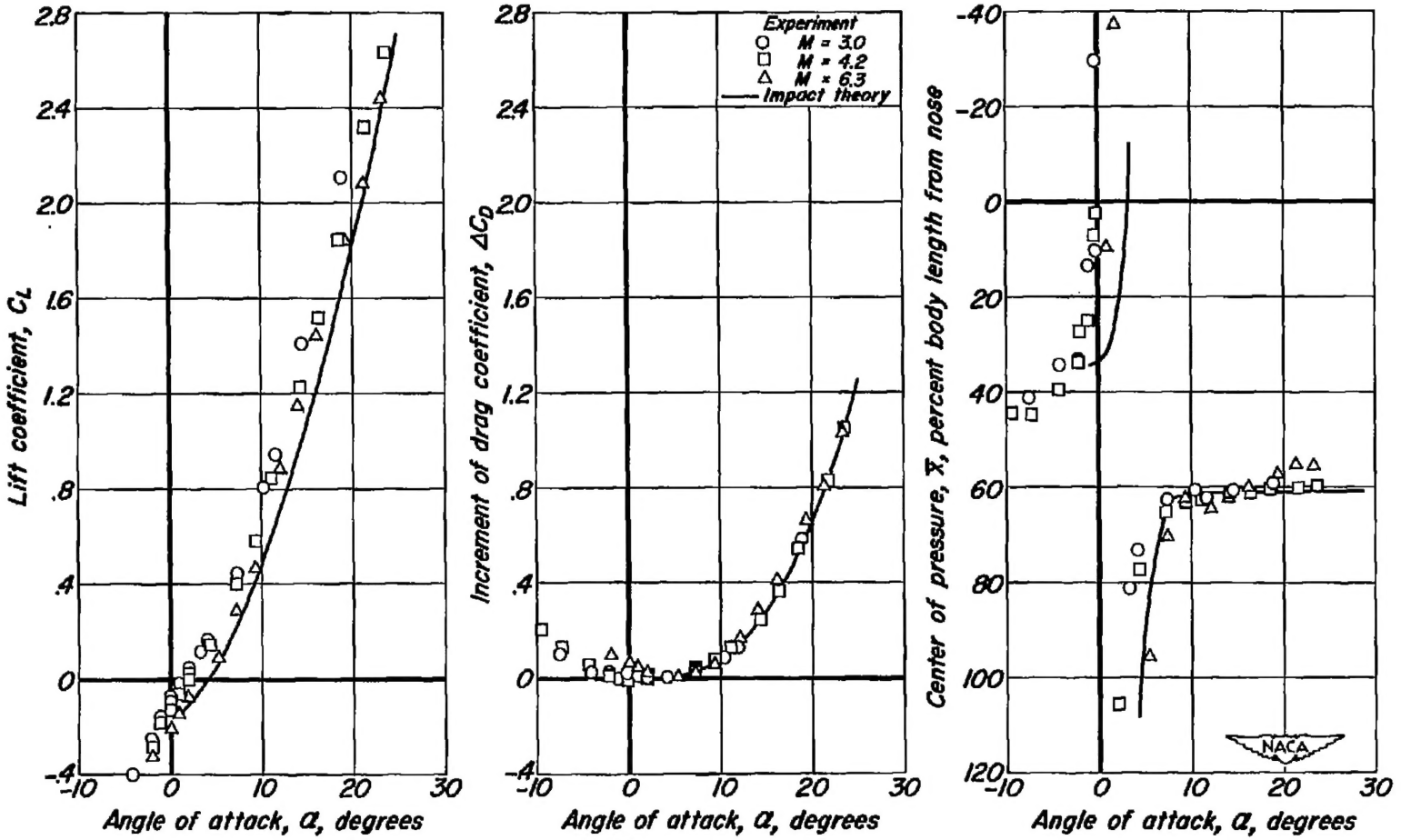

(b) $f_n = 5$, $f_a = 5$

Figure 16.– Continued.

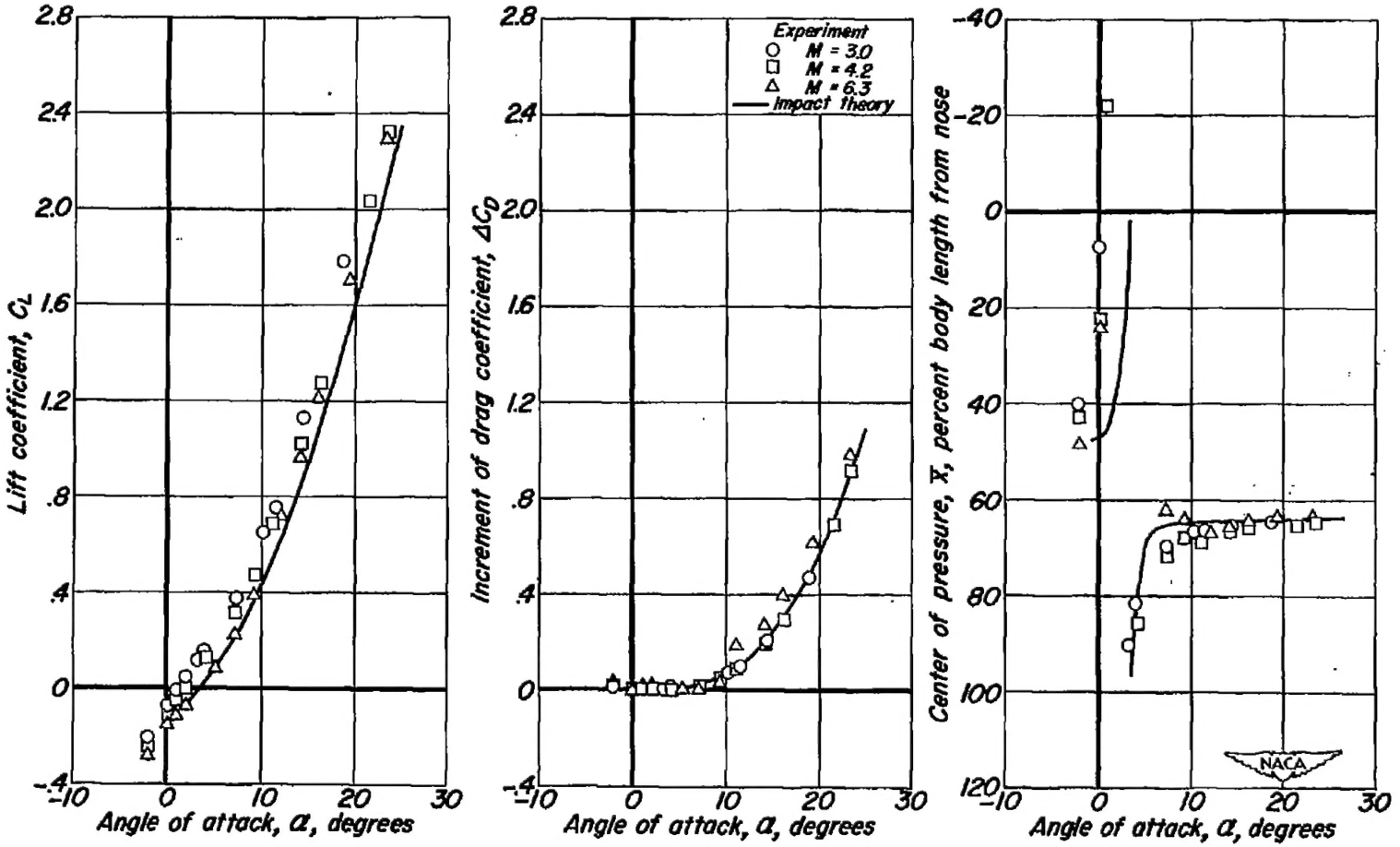

(c) $f_n = 7$, $f_a = 3$

Figure 16.– Concluded.